Article

A dynastic elite in monumental Neolithic society

Lara M. Cassidy[1 ✉], Ros Ó Maoldúin[1,2,3], Thomas Kador[4], Ann Lynch[5], Carleton Jones[6], Peter C. Woodman[7,13], Eileen Murphy[8], Greer Ramsey[9], Marion Dowd[10], Alice Noonan[1], Ciarán Campbell[1], Eppie R. Jones[1,11,12], Valeria Mattiangeli[1] & Daniel G. Bradley[1 ✉]

The nature and distribution of political power in Europe during the Neolithic era remains poorly understood[1]. During this period, many societies began to invest heavily in building monuments, which suggests an increase in social organization. The scale and sophistication of megalithic architecture along the Atlantic seaboard, culminating in the great passage tomb complexes, is particularly impressive[2]. Although co-operative ideology has often been emphasised as a driver of megalith construction[1], the human expenditure required to erect the largest monuments has led some researchers to emphasize hierarchy[3]—of which the most extreme case is a small elite marshalling the labour of the masses. Here we present evidence that a social stratum of this type was established during the Neolithic period in Ireland. We sampled 44 whole genomes, among which we identify the adult son of a first-degree incestuous union from remains that were discovered within the most elaborate recess of the Newgrange passage tomb. Socially sanctioned matings of this nature are very rare, and are documented almost exclusively among politico-religious elites[4]— specifically within polygynous and patrilineal royal families that are headed by god-kings[5,6]. We identify relatives of this individual within two other major complexes of passage tombs 150 km to the west of Newgrange, as well as dietary differences and fine-scale haplotypic structure (which is unprecedented in resolution for a prehistoric population) between passage tomb samples and the larger dataset, which together imply hierarchy. This elite emerged against a backdrop of rapid maritime colonization that displaced a unique Mesolithic isolate population, although we also detected rare Irish hunter-gatherer introgression within the Neolithic population.

Previous analyses of ancient genomes have demonstrated common ancestry between the societies of the Atlantic seaboard during the Neolithic[7–9], while recent modelling of radiocarbon determinations has defined repeat expansions of megalithic architecture from northwest France at a pace that implies more advanced maritime technology than was previously assumed for these regions[10]. This includes the spread of passage tombs along the Atlantic façade during the fourth millennium BC—a period that also saw the arrival of agriculture in Ireland, alongside other distinct megalithic traditions. These structures reached some of the highest concentrations and diversities known for Europe on the island of Ireland. However, the political systems that underlay these societies remain obscure, as does the genetic input from indigenous Mesolithic hunter-gatherers.

To investigate these issues, we shotgun-sequenced individuals dating to the Irish Mesolithic ($n = 2$) and Neolithic ($n = 42$) periods to a median 1.14× coverage (Fig. 1a, Supplementary Tables 1, 2). We imputed 43 of

these individuals alongside relevant ancient genomes (Supplementary Table 3), including an additional 20 British and Irish individuals[7,9,11]. We then merged these individuals with a published dataset of imputed ancient genotypes[12] to allow for fine-scale haplotypic inference of population structure[13] and estimations of inbreeding. Four key individuals were subsequently sequenced to higher (13–20×) coverage.

We sampled remains from all of the major Irish Neolithic funerary traditions: court tombs, portal tombs, passage tombs, Linkardstown-type burials and natural sites (Fig. 1a, c, Supplementary Information section 1). Within this dataset, the earliest Neolithic human remains from the island—interred at Poulnabrone portal tomb[14]—are of majority 'Early_Farmer' ancestry (as defined by ADMIXTURE modelling[15]), and show no evidence of inbreeding (Fig. 1a, Extended Data Fig. 1), which implies that, from the very onset, agriculture was accompanied by large-scale maritime colonization. Our ADMIXTURE and ChromoPainter[13] analyses do not distinguish between the Irish and British Neolithic

[1]Smurfit Institute of Genetics, Trinity College Dublin, Dublin, Ireland. [2]The Irish Fieldschool of Prehistoric Archaeology, National University of Ireland Galway, Galway, Ireland. [3]Archaeological Management Solutions, Kilrush, Ireland. [4]UCL Arts and Sciences, University College London, London, UK. [5]National Monuments Service, Department of Culture, Heritage and the Gaeltacht, Dublin, Ireland. [6]School of Geography, Archaeology, and Irish Studies, National University of Ireland Galway, Galway, Ireland. [7]Department of Archaeology, University College Cork, Cork, Ireland. [8]Archaeology and Palaeoecology, School of Natural and Built Environment, Queen's University Belfast, Belfast, UK. [9]National Museums NI, Cultra, UK. [10]CERIS, School of Science, Institute of Technology Sligo, Sligo, Ireland. [11]Department of Zoology, University of Cambridge, Cambridge, UK. [12]Genomics Medicine Ireland, Dublin, Ireland. [13]Deceased: Peter C. Woodman. ✉e-mail: cassidl1@tcd.ie; DBRADLEY@tcd.ie
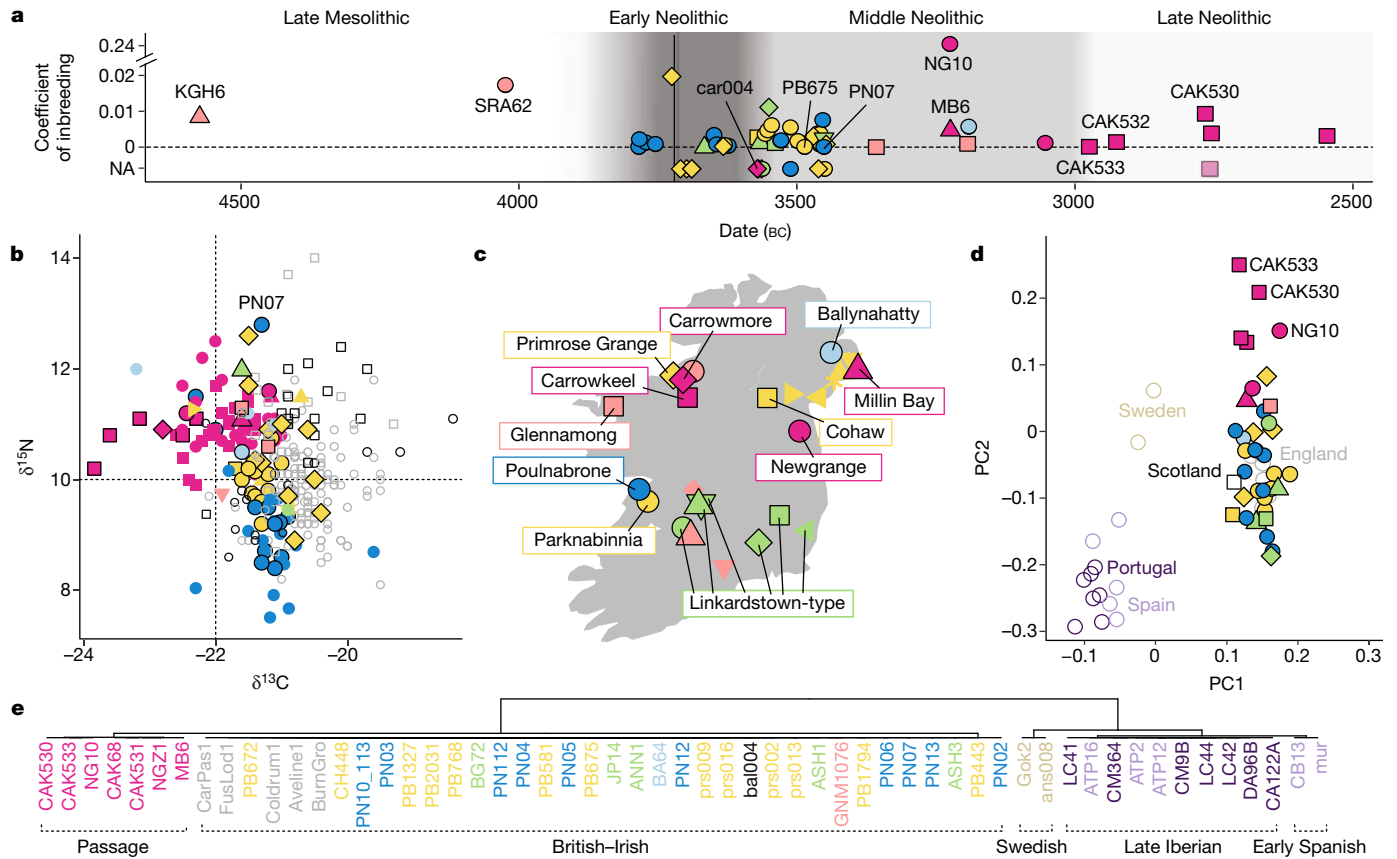
Fig. 1 | Fine-scale haplotypic and dietary structure in the Neolithic.
a, Timeline of analysed Irish genomes with inbreeding coefficients are shown for those with sufficient coverage. All dates are direct and calibrated, excluding that for individual CAK534 (translucent). The key for the sample sites is given in **c**. The earliest widespread evidence of Neolithic activity (house horizon) is marked with a black line. The Irish Neolithic ends at about 2500 BC. NA, not applicable.
b, Stable isotope values for samples from the Irish and British Neolithic (*n* = 292). The key for the Irish samples is given in **c**, and samples included in the ancient DNA analysis are outlined in black. British samples are shown as hollow shapes; black, Scotland; grey, England or Wales; circles, pre-3400 BC; squares, post-3400 BC. An infant with Down syndrome (PN07) is labelled; this individual showed isotope values consistent with a high trophic level. **c**, Site locations for Irish individuals sampled or included in this study coloured by burial type: yellow, court tomb; blue, portal tomb; green, Linkardstown-type; magenta, passage tomb and related; light pink, natural sites; and light blue, the unclassified Ballynahatty[7] megalith. Sites outlined in black were included in ancient DNA analysis. **d**, ChromoPainter[13] principal component (PC) analysis of individuals from the Atlantic seaboard of majority Early_Farmer ancestry (*n* = 57), generated using a matrix of haplotypic length-sharing. Passage tomb outliers in Fig. 2d are labelled. **e**, fineSTRUCTURE dendrogram derived from the same matrix as in **d** with five consistent clusters.

populations (Fig. 1d, Extended Data Figs. 1, 2). They also confirm previous reports[7,8] that samples from the Early Neolithic of Spain are the best proxy source of their Early_Farmer ancestry (Extended Data Fig. 1), which emphasizes the importance of Atlantic and Mediterranean waterways in their forebearers' expansions.

Overall, no increase in inbreeding is seen through time in Neolithic Ireland, which indicates that communities maintained sufficient size and communication to avoid matings between relatives of the fifth degree or closer (Fig. 1a). However, we report a single extreme outlier interred within the Newgrange passage tomb—a focal point of the monumental landscape of Brú na Bóinne, a United Nations Educational, Scientific and Cultural Organization world heritage site (Fig. 2a). Incorporating over 200,000 tonnes of earth and stone, this megalithic mound is one of the most spectacular of its kind known from Europe[16]. Although externally designed for public consumption, the interior of the tomb consists of a single narrow passage with a specialized ritual inventory, the winter-solstice solar alignment of which would have been viewed by only a select few. Unburnt, disarticulated human bone was found[16] concentrated within the most elaborately decorated recess of the terminal cruciform chamber, including the cranial remains of an adult male (designated NG10) (Fig. 2b, Supplementary Information section 1.4.1). The exceptional location of these remains is matched by a

genomic heritage that—to our knowledge—is unprecedented in ancient genomics. He possessed multiple long runs of homozygosity, each comprising large fractions of individual chromosomes (Fig. 2e, Extended Data Fig. 3a), and totalling to a quarter of the genome (inbreeding coefficient = 0.25). This marks him as the offspring of a first-order incestuous union, which is a near-universal taboo for entwined biological and cultural reasons[4]. However, given the nature of the interment, his parentage was very likely to have been socially sanctioned.

Although simulations cannot distinguish whether his parents were full siblings or parent and offspring (Extended Data Fig. 3), the only known definitive acceptances of such mating occur among siblings—specifically within polygynous elites—as part of a rarely observed phenomenon known as 'royal' or 'dynastic' incest[4,6,17]. In all of these documented cases (for example, in pre-contact Hawai'i, the Inca empire and ancient Egypt)[5,6], this behaviour co-occurs with the deification of political leaders and is typically limited to ruling families, whose perceived divinity exempts them from social convention. Both full sibling and half-sibling marriages are found most commonly in complex chiefdoms and early states; researchers have generally viewed them as a means of intensifying hierarchy and legitimizing power in the absence of more advanced bureaucratic systems, alongside tactics such as extravagant monumental architecture and public ritual[18–20].
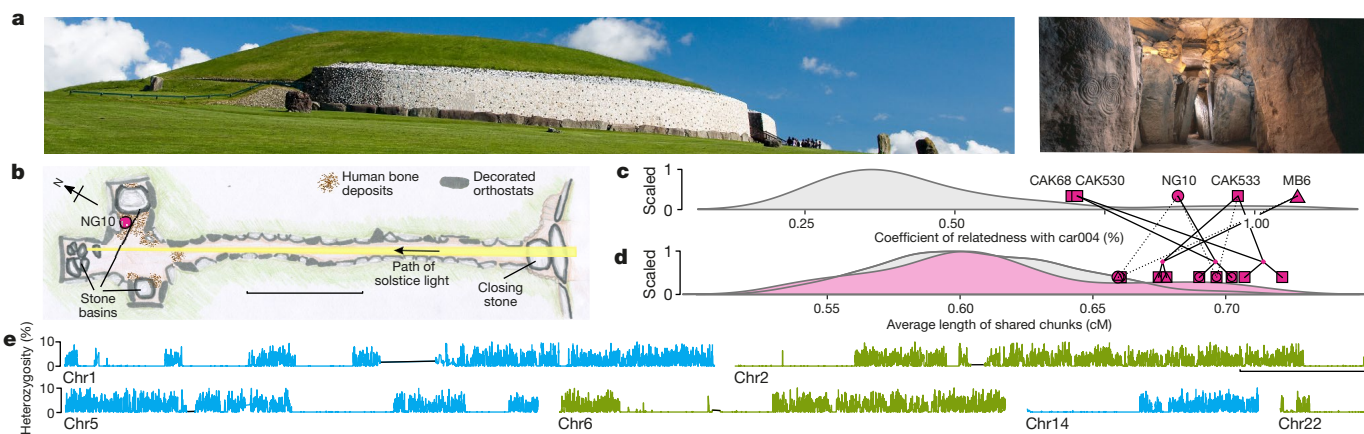
Fig. 2 | Genomic signals of dynasty among focal passage tomb interments.
a, Front elevation and interior of the Newgrange passage tomb. Photographs by Fáilte Ireland; Photographic Unit, National Monuments Service. **b**, Plan of chamber, redrawn after ref. [16]. Scale bar, 6 m. **c**, The coefficient of relatedness (pi-HAT) between car004 (an interment from the central monument at Carrowmore)[9], and 38 British and Irish Neolithic samples, with the top 5 hits labelled (CAK68 and CAK530 are equal in value). **d**, Average length of donated haplotypic chunks between all reciprocal pairs of the 'passage tomb cluster'

(pink; $n = 42$) and 'British–Irish cluster' (grey; $n = 1,190$) as defined by fineSTRUCTURE in Fig. 1e. The highest values for passage-tomb-cluster pairs are marked along the x axis, with an excess of longer chunks shared between the inferred kin of car004 (CAK533, MB6 and NG10) in **c**. Darker lines link reciprocal donations. Combined symbols are used for inter-site pairs. **e**, A sliding window of heterozygosity is plotted for transversions along selected chromosomes of NG10, revealing extreme runs of homozygosity. Scale bar, 50 Mb.

We propose that a comparable set of social dynamics was in operation in Ireland by the Middle Neolithic, and—given that solstice-aligned passage tombs similar to Newgrange were constructed in Wales, Orkney and Brittany[21]—may have occurred outside the island as well. Notably, levels of consanguinity are consistently low and decrease through time across our wider dataset of imputed ancient genomes (Extended Data Fig. 4); we detected only one other incidence of close inbreeding, the son of second- or third-degree relatives from a Swedish megalith[9].

The Brú na Bóinne passage tombs appear in Medieval mythology that relates their construction to magical manipulations of the solar cycle by a tribe of gods, which has led to unresolved speculation about the durability of oral traditions across millennia[22]. Although such longevity seems unlikely, our results strongly resonate with mythology that was first recorded in the eleventh century AD, in which a builder-king restarts the daily solar cycle by copulating with his sister[23]. Fertae Chuile, a Middle Irish placename for the Dowth passage tomb (which neighbours Newgrange), is based on this lore, and can be translated as 'Hill of Sin' or 'Hill of Incest'[23,24].

A second centre of the passage tomb tradition is found 150 km to the west of Newgrange, near the Atlantic coast. This centre comprises the mega-cemeteries of Carrowmore and Carrowkeel, which have origins that pre-date the construction of Newgrange by several centuries; depositions at Carrowkeel continued until at least the end of the Neolithic[25]. Using analyses based on both single-nucleotide polymorphisms (SNPs) and haplotypes, we uncover a web of relatedness that connects these sites to both Newgrange and the atypical Millin Bay megalith on the northeast coast, which has previously been recognized as part of the broader passage tomb tradition on the basis of its artwork and morphological features (Supplementary Information section 1.4.3).

First, using lcMLkin[26] (Fig. 2c), we find that the earliest passage tomb genome in the dataset (designated car004 (ref. [9]))—interred within the focal monument at Carrowmore—has detectable distant kinship with NG10, as well as with other later individuals from Carrowkeel and Millin Bay (designated CAK533 and MB6, respectively). A similar kinship coefficient (≥6th degree) is also seen between NG10 and another individual from Carrowkeel (designated CAK532) (Extended Data Fig. 5a), demonstrating familial ties between several of the largest hubs of the tradition.

Second, in our fineSTRUCTURE[13] analysis of genomes from the Atlantic seaboard of majority Early_Farmer ancestry, samples from

Newgrange, Carrowkeel and Millin Bay form a distinct cluster that is split from a larger British and Irish grouping (Fig. 1d, e). We confirmed the robustness of this cluster using a larger dataset of ancient genomes (Extended Data Fig. 2). Our ChromoPainter[13] analysis also identifies excessive reciprocal haplotype donation specifically between NG10 and CAK532, which confirms their kinship (Extended Data Fig. 5b). We found evidence of more-distant relatedness between the inferred relatives of car004 (ref. [9]), who share elongated haplotypic chunks with one another; this signature of recent shared ancestry also links a third individual from Carrowkeel (designated CAK530) to CAK533 and NG10 (Fig. 2d, labelled on Fig. 1d).

The earlier car004 (ref. [9]) genome is of low coverage (0.04×), and thus was excluded from our ChromoPainter analysis. However, D-statistics demonstrate that this sample preferentially forms a clade with the passage tomb cluster ($Z > 3.4$) (Supplementary Table 10), despite being closer in time to the majority of samples from the larger British and Irish cluster. Moreover, this attraction is only partially driven by the aforementioned kin connections, which we further corroborate. Downsampling tests on the larger dataset demonstrate that the D-statistic results for car004 are highly significant (Supplementary Table 11).

Taken together, we favour the interpretation that the haplotypic structure within our dataset is driven by excessive identity-by-descent sharing between passage tomb samples, which implies non-random mating across large territories of the island. A high degree of social complexity would be required to achieve this, as is predicted by the parentage of NG10. However, our genomes from non-passage-tomb interments are largely earlier in date and a denser sampling of diverse sites from the Late Neolithic will be required to evaluate the contribution of temporal drift to the fineSTRUCTURE clustering. Stable isotope values also differentiate passage tomb interments from other Irish and British Neolithic samples (Fig. 1b). The combination of high $\delta^{15}N$ and depleted $\delta^{13}C$ values in passage tomb remains is best explained by a diet of meat and animal products (associated with privilege), although it remains to be seen how this relates to broader dietary change during the period.

The simpler court and portal tombs lack the artwork and prestigious grave goods of the passage tomb tradition, and are arguably a manifestation of smaller-scale, lineage-based societies[3]. These architectures do not typically occur within cemeteries of passage tombs—although exceptions do exist, including a court tomb constructed beside
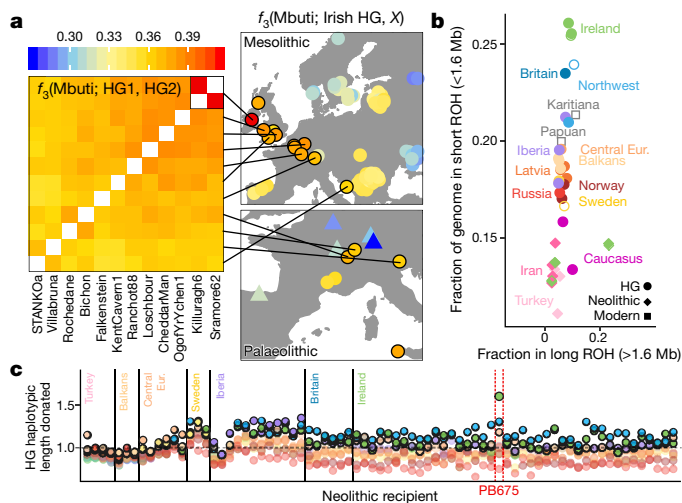
Fig. 3 | Origins and legacy of the Irish Mesolithic. a, Right, the maps show the estimates of shared drift between Irish and British or continental hunter-gatherers (HG) (jittered) from the Mesolithic and Upper Palaeolithic (triangles, Magdalenian culture). Left, the top ten hits with sufficient coverage are cross-compared with one another and with Irish hunter-gatherers in a heat map using the statistic f_3(Mbuti; HG1, HG2), in which HG1 and HG2 represent all possible pairs. **b**, Short and long runs of homozygosity (ROH) spectra in modern and ancient genomes. Hollow shapes indicate direct (rather than imputed) diploid calls. For four Irish samples, both imputed and direct data are presented, showing close agreement. **c**, Normalized haplotypic length donations from hunter-gatherer populations to Neolithic individuals, arranged by their geographic region (labelled). The top three hunter-gatherer donors are outlined for each individual. Donor hunter-gatherer population colours are as in **b**; British and northwestern European hunter-gatherers are merged into one donor population (blue).

Carrowmore with a reported instance of inter-site kinship[9]. We find evidence of both distant kinship (Supplementary Information section 6.5) and societal structure between another pair of distinct, but neighbouring, megaliths (10 km apart)—the Poulnabrone portal tomb[14] and the Parknabinnia court tomb[27]. Their sampled cohorts (the majority of which are males) show a significant difference in the frequency of two Y chromosome haplogroups ($P = 0.035$, Fisher's exact test), as well as a dietary difference (Fig. 1b, Extended Data Fig. 6). Given that there is a lack of close kin within either tomb, we exclude small family groups as their sole proprietors and interpret our findings as the result of broader social differentiation with an emphasis on patrilineal descent. The double occurrence of a rare Y haplogroup (H2a) among the individualized male Linkardstown burials of the southeast of the island provides further evidence of the importance of patrilineal ancestry in these societies[9], as does the predominance of a single Y haplogroup (I-M284) across the Irish and British Neolithic population (Extended Data Fig. 7).

It has previously been hypothesized that the spread of agriculture into Britain and Ireland was assisted by pre-existing maritime connections that developed in the Mesolithic[28]. However, our results suggest that, before the Neolithic, the Irish Sea posed a formidable barrier to gene flow. The genomes of Irish hunter-gatherers form a distinct cluster within a wider grouping of Mesolithic hunter-gatherers from northwest Europe[11,29,30], sharing excessive levels of drift with each other despite a separation of over half a millennium (Fig. 3a, Extended Data Fig. 2, Supplementary Information section 4.1). By contrast, British hunter-gatherers show no differentiation from their continental contemporaries[11]. This is consistent with palaeogeographic models that posit a Doggerland bridge between Britain and the continent for most of the Mesolithic, but a separation of Ireland that pre-dates the Holocene epoch[31].

To our knowledge, Irish hunter-gatherers also exhibit the largest degree of short runs of homozygosity (Fig. 3b) described for any ancient—or indeed modern—genome, a signature of ancestral constriction that supports a prolonged period of island isolation. This implies that continental and British hunter-gatherers lacked the technology or impetus required to maintain frequent contact with Ireland, and reflects the relatively late seaborne colonization of the island in the Mesolithic (approximately 8,000 BC), followed by a sharp divergence in lithic assemblages[32]. Nonetheless, as there were no signatures of recent inbreeding (Fig. 1a), it appears Irish hunter-gatherers were capable of sustaining outbreeding networks within the island itself despite the estimated carrying capacity of only 3,000–10,000 individuals[32].

Ultimately, Irish hunter-gatherers originate from sources who are related to individuals of the Upper Palaeolithic period from Italy[29] (Fig. 3a), and show no evidence of contribution from an earlier western lineage that persisted in Spain[33]. However, we detect a significant excess of this ancestry in a hunter-gatherer of the Mesolithic from Luxembourg[30] relative to Irish and British hunter-gatherers (Supplementary Table 9), demonstrating the survival of this ancestry outside Iberia. We also explore the genetic legacy of Irish hunter-gatherers in the Neolithic population of the island, and discover an incidence of direct ancestral contribution. Within a broader pattern of high haplotypic affinities among European farmers to local hunter-gatherer groups (Fig. 3c), we uncover an outlier from Parknabinnia court tomb (designated PB675) who shows a disproportionate and specifically Irish hunter-gatherer contribution. High variance in hunter-gatherer ancestry across the genome and an excess of elongated Irish hunter-gatherer haplotypes in this individual support a recent introgression (Extended Data Fig. 8) that we estimate to have been within four generations (Supplementary Information section 3).

This finding, combined with evidence of local hunter-gatherer input into Neolithic populations in Scotland[11], implies recurring interactions between incoming farmers and the indigenous populations of Britain and Ireland. Notably, an approximately fourth-degree relative of PB675 was interred within the same tomb (Extended Data Fig. 5a), which implies that this genetic outlier was integrated within the community. An alternate instance of diversity in those selected for megalithic interment is seen in a male infant from Poulnabrone (designated PN07) with a dietary signature of breastfeeding (Fig. 1b, Extended Data Fig. 6). This individual has a clear trisomy of chromosome 21, which—to our knowledge—constitutes the earliest definitive discovery of a case of Down syndrome (pre-dating previous evidence from the fifth to sixth centuries AD[34]).

Overall, our results demonstrate the capacity of ancient genomes to shed light not only on population movements, but also on political systems and social values where no written records exist. This is particularly true when imputation and haplotypic analyses are used, which we here affirm outperform popular methods based on SNPs in the resolution of ancient population structure (Extended Data Fig. 9). Together with estimations of inbreeding and kinship, these methods broaden the scope within which we can study the development of agricultural societies from small chiefdoms to civilizations. Specifically, our findings support a re-evaluation of social stratification and political integration in the megalithic cultures of the Atlantic seaboard[10], and suggest that the passage-tomb-building societies of Ireland possessed several attributes found within early states and their precursors.

Online content

Any methods, additional references, Nature Research reporting summaries, source data, extended data, supplementary information, acknowledgements, peer review information; details of author contributions and competing interests; and statements of data and code availability are available at https://doi.org/10.1038/s41586-020-2378-6.

Article

1. Hinz, M., Müller, J. & Wunderlich, M. in *Megaliths, Societies, Landscapes: Early Monumentality and Social Differentiation in Neolithic Europe* Vol. 1 (eds Hinz, M. et al.) 21–23 (Habelt, 2019).
2. Cunliffe, B. *Facing the Ocean: the Atlantic and its Peoples* (Oxford Univ. Press, 2004).
3. Burenhult, G. Megalithic symbolism in Ireland and Scandinavia in light of new evidence from Carrowmore. *Arkeos* **6**, 49–108 (1999).
4. Wolf, A. P. *Incest Avoidance and the Incest Taboos: Two Aspects of Human Nature* (Stanford Univ. Press, 2014).
5. Goggin, J. M. & Sturtevant, W. P. in *Explorations in Cultural Anthropology. Essays in Honour of George Peter Murdock* (ed. Goodenough, W. H.) 179–219 (McGraw-Hill, 1964).
6. van den Berghe, P. L. & Mesher, G. M. Royal incest: a reply to Sturtevant. *Am. Ethnol.* **8**, 187–188 (1981).
7. Cassidy, L. M. et al. Neolithic and Bronze Age migration to Ireland and establishment of the insular Atlantic genome. *Proc. Natl Acad. Sci. USA* **113**, 368–373 (2016).
8. Olalde, I. et al. The Beaker phenomenon and the genomic transformation of northwest Europe. *Nature* **555**, 190–196 (2018).
9. Sánchez-Quinto, F. et al. Megalithic tombs in western and northern Neolithic Europe were linked to a kindred society. *Proc. Natl Acad. Sci. USA* **116**, 9469–9474 (2019).
10. Schulz Paulsson, B. Radiocarbon dates and Bayesian modeling support maritime diffusion model for megaliths in Europe. *Proc. Natl Acad. Sci. USA* **116**, 3460–3465 (2019).
11. Brace, S. et al. Ancient genomes indicate population replacement in Early Neolithic Britain. *Nat. Ecol. Evol.* **3**, 765–771 (2019).
12. Martiniano, R. et al. The population genomics of archaeological transition in west Iberia: investigation of ancient substructure using imputation and haplotype-based methods. *PLoS Genet.* **13**, e1006852 (2017).
13. Lawson, D. J., Hellenthal, G., Myers, S. & Falush, D. Inference of population structure using dense haplotype data. *PLoS Genet.* **8**, e1002453 (2012).
14. Lynch, A. *Poulnabrone: An Early Neolithic Portal Tomb in Ireland* (Stationery Office, 2014).
15. Alexander, D. H., Novembre, J. & Lange, K. Fast model-based estimation of ancestry in unrelated individuals. *Genome Res.* **19**, 1655–1664 (2009).
16. O'Kelly, M. J. *Newgrange* (Thames & Hudson, 1983).
17. Huebner, S. R. 'Brother–sister' marriage in Roman Egypt: a curiosity of humankind or a widespread family strategy? *J. Roman Stud.* **97**, 21–49 (2007).
18. Kolb, M. J. et al. Monumentality and the rise of religious authority in precontact Hawai'i. *Curr. Anthropol.* **35**, 521–547 (1994).
19. Gates, H. in *Inbreeding, Incest, and the Incest Taboo: The State of Knowledge at the Turn of the Century* (eds Wolf, A. P. & Durham, W. H.) 139–160 (Stanford Univ. Press, 2005).
20. Kirch, P. V. *How Chiefs Became Kings: Divine Kingship and the Rise of Archaic States in Ancient Hawai'i* (Univ. California Press, 2010).
21. Hensey, R. *First Light: The Origins of Newgrange* (Oxbow Books, 2015).
22. Hensey, R. in *The Oxford Handbook of Light in Archaeology* (eds Papadopoulos C. & Moyes H.) (Oxford Univ. Press, 2017).
23. Carey, J. Time, memory, and the Boyne necropolis. *Proc. Harv. Celtic Colloq.* **10**, 24–36 (1990).
24. Gwynn, E. *The Metrical Dindshenchas. 4. Text, Translation, and Commentary* (School of Celtic Studies, Dublin Institute for Advanced Studies, 1991).
25. Kador, T. et al. Rites of passage: mortuary practice, population dynamics, and chronology at the Carrowkeel passage tomb complex, Co. Sligo, *Ireland. Proc. Prehist. Soc.* **84**, 225–255 (2018).
26. Lipatov, M., Sanjeev, K., Patro, R. & Veeramah, K. Maximum likelihood estimation of biological relatedness from low coverage sequencing data. Preprint at https://www.biorxiv.org/content/10.1101/023374v1 (2015).
27. Jones, C. in *Megaliths, Societies, Landscapes: Early Monumentality and Social Differentiation in Neolithic Europe* Vol. 18 (eds Müller, J. et al.) 979–1000 (Habelt, 2019).
28. Garrow, D. & Sturt, F. Grey waters bright with Neolithic argonauts? Maritime connections and the Mesolithic–Neolithic transition within the 'western seaways' of Britain, *c.* 5000–3500 BC. *Antiquity* **85**, 59–72 (2011).
29. Fu, Q. et al. The genetic history of Ice Age Europe. *Nature* **534**, 200–205 (2016).
30. Lazaridis, I. et al. Ancient human genomes suggest three ancestral populations for present-day Europeans. *Nature* **513**, 409–413 (2014).
31. Brooks, A. J., Bradley, S. L., Edwards, R. J. & Goodwyn, N. The palaeogeography of Northwest Europe during the last 20,000 years. *J. Maps* **7**, 573–587 (2011).
32. Woodman, P. *Ireland's First Settlers: Time and the Mesolithic* (Oxbow Books, 2015).
33. Villalba-Mouco, V. et al. Survival of Late Pleistocene hunter-gatherer ancestry in the Iberian peninsula. *Curr. Biol.* **29**, 1169–1177.e7 (2019).
34. Rivollat, M., Castex, D., Hauret, L. & Tillier, A.-M. Ancient Down syndrome: an osteological case from Saint-Jean-des-Vignes, northeastern France, from the 5–6th century AD. *Int. J. Paleopathol.* **7**, 8–14 (2014).

Methods

No statistical methods were used to predetermine sample size. The experiments were not randomized and investigators were not blinded to allocation during experiments and outcome assessment.

Sampling and sequencing

We sampled 54 petrous temporal bones and 12 teeth (Supplementary Table 1) sourced from 20 archaeological sites (Supplementary Information section 1). Two of these, PN10 and PN113, were later found to belong to the same individual. Processing was carried out in clean-room facilities dedicated to ancient DNA research at Trinity College Dublin. Photographs were taken before sample alteration, and these are available upon request to the corresponding authors. The dense otic capsule region of petrous bones and the root cementum of teeth were targeted for sampling. Bone or tooth powder (130–150 mg) was subjected to a previously described silica-column method[35] of DNA extraction with modifications[36]. Three successive extractions were performed on samples (incubation times of 24 h at 37 °C). Five samples were subjected to a modified protocol, in which the powder was first washed twice with EDTA (0.5 M) and then subjected to a single extraction (incubation time of 48 h at 37 °C).

Select sample extracts (typically the third) were purified at a volume of 55 μl and Illumina next-generation-sequencing double-stranded libraries were created from 16.50-μl aliquots, following previously described methods[7,37] that are based on an established protocol[38]. Library amplification reactions were carried out using Accuprime Pfx Supermix (Life Technology), primer IS4 (0.2 μM), a specific indexing primer (0.2 μM) and 3 μl of library as previously described[7], and DNA concentrations assessed on an Agilent 2100 Bioanalyzer or 2200 Tapestation. Amplified libraries were first screened for endogenous human content on an Illumina MiSeq platform (TrinSeq, Trinity College Dublin) using 65- or 70-bp single-end sequencing. Extracts with sufficient human endogenous content (>5%) and concentration (>0.5 ng/μl at 12 PCR cycles) were incubated with USER enzyme (volume of 5 μl to 16.50 μl of extract) for 3 h at 37 °C to repair post-mortem molecular damage. Following this, library creation and amplification was carried out as described above. USER-treated libraries from a total of 45 individuals were sent for higher coverage sequencing at Macrogen (100-bp single-end with the exception of JP14, for which 100-bp paired-end data were also obtained). Detailed experimental and sequencing results can be found in Supplementary Table 2.

Demultiplexed data returned in FASTQ format were subjected to quality control using the FastQC suite[39]. Residual adaptor sequences were trimmed using cutadapt v.1.2.1[40], with non-default parameters -m 34 and -O 1. Quality trimming was performed on read ends where necessary. Paired-end reads from JP14 were collapsed and trimmed for adapters using the leeHom software[41]. Trimmed reads were mapped to hg19/GRCh37 with the mitochondrial genome replaced with the revised Cambridge reference sequence (NC_012920.1). BWA version 0.7.5[42] was used for alignment with non-default parameters -l 16500, -n 0.02 and -o 2. Reads were sorted, filtered for a mapping quality of 20 or above and PCR duplicates removed using Samtools v.0.1.19[43]. Read groups were added and BAM files merged to sample level using Picard Tools v.1.101 (http://broadinstitute.github.io/picard/). GenomeAnalysisTK v.2.4-7[44] was used to locally realign reads. Two base pairs at both the 5′ and 3′ ends of reads had their base qualities reduced to a PHRED score of 2. Where necessary, published ancient genomic data[7,8,11,12,29,37,45–71] were realigned for use in downstream analyses from either unaligned FASTQ (when available) or aligned BAM files following the parameters described here, and filtered in an identical manner.

Radiocarbon dating and isotope analysis

Direct radiocarbon dates were obtained for 27 samples from accelerator mass spectrometry facilities at Queen's University Belfast and the University of Oxford. All calibrated dates are taken from CALIB 7.1 after ref. [72] using the IntCal13 curve, and reported at two standard deviations (95.4% confidence). The median probabilities (calibrated BC) have been used for plotting samples chronologically. Stable isotope ratios ($\delta^{13}C$ and $\delta^{15}N$) are also reported for the 27 samples and compared with published stable isotope data from 85 Irish and 81 British samples[8,9,11,14,25,69,73–90] (Fig. 1, Supplementary Table 4). The timeline in Fig. 1 is phased following ref. [91].

Molecular sexing and aneuploidy detection with read coverage

Molecular sexing was done following two methods, one previously published[92] and one described as follows. The total number of X chromosome reads was divided by the length of the X chromosome. This value was then divided by the median seen for the same calculation across the autosomal chromosomes. We call this value Rx: a value above 0.9 was designated female, and a value below 0.6 was designated as male (Supplementary Table 5). Chromosomal deletions or duplications of sufficient length can be detected by aberrations in read coverage for shotgun data. We estimated the chromosomal coverages for 145 shotgun-sequenced ancient individuals and 43 samples from the current study (>0.3× mean genome coverage) using Qualimap[93]. To compare chromosomal coverage between samples, we normalized values by the mean autosomal coverage for each genome. An extreme outlier was observed for chromosome 21. To estimate the aberration in read coverage for this sample, we divided its normalized chromosome 21 coverage by the median for this value seen across all samples (Extended Data Fig. 6b).

Mitochondrial analysis

To determine mitochondrial coverage and haplogroups, reads aligned (no mapping quality filter) to the human reference genome and revised Cambridge mitochondrial reference sequence were realigned to the mitochondrial reference alone and re-processed as described in 'Sampling and sequencing'. Coverages were obtained using Qualimap v.2.1.1[93]. Consensus sequences were determined as previously described[47] with Samtools mpileup (-B, -d6 and -Q 30) and vcfutils.pl (vcf2fq)[43]. HaploFind[94] was used to identify defining mutations and assign haplogroups (Supplementary Table 6). Mitochondrial contamination was estimated as previously described[7,63]. Sequence data from the original alignment (hg19 and the revised Cambridge reference sequence) were used for contamination estimates, to avoid the confounding effects of misaligned NUMT sequences. Contamination estimates with and without the inclusion of potential damage sites are given (Supplementary Table 6).

Genotype calling

As the majority of published ancient genomic data possess sequencing coverages too low for direct diploid genotype calling, two alternative methods were used—pseudo-haploid genotype calling and genotype imputation. To minimize the effect of reference bias previously observed in pseudo-haplodized data[12], a relaxed mapping quality filter of 20 was applied during data processing. Randomized pseudo-haploid genotypes (base quality >30) were called following previously established methods[7]. Imputation was carried out using Beagle 4.0[95] for 43 individuals from the current study (>0.4×) (Supplementary Table 2), and 51 published[7,9,11,29,54,56–58,60,64,65,96] ancient genomes (>0.66×) (Supplementary Table 3), following previously published methods[12,37,51,59] with some modifications as indicated below.

Genotype likelihoods for biallelic autosomal SNPs in the 1000 Genomes phase 3 dataset[97] were called using the UnifiedGenotyper tool in GenomeAnalysisTK v.2.4-7[44]. These genotypes were then filtered to add equal likelihoods for missing data and for genotypes that could be the result of post-mortem damage. Samples were merged by chromosome and imputed in 15,000 marker windows using the 1000 Genomes phase 3 haplotypic reference panel and genetic map files provided

Article

by the BEAGLE website (http://bochet.gcc.biostat.washington.edu/beagle/). To assess accuracy, imputed genotypes for chromosome 22 of the downsampled Neolithic NE1[37] genome (1×), were compared to direct diploid genotypes from the high-coverage version (25×) (Extended Data Fig. 10). Optimal filters of >0.05 minor allele frequency, >0.99 genotype probability and exclusion of transition sites were subsequently chosen for all downstream analysis. Six individuals—including three from the current study (ANN2, PB754 and PN16)—were excluded from downstream analysis owing to a high percentage of genotype missingness (>0.16) after the imposition of the genotype probability filter. The remaining 88 individuals were combined with published imputed genotypes (filtered identically) from 67 ancient samples[12].

Direct diploid genotype calling was also carried out for high-coverage ancient genomes (>10×) at positions in the 1000 Genomes phase 3 variant panel using the HaplotypeCaller tool in GenomeAnalysisTK v.4.0[44] with parameter -mbq 30. A minimum genotype quality of 30, a minimum depth of coverage of 10×, and a maximum depth of coverage twice that of the mean genomic coverage of the sample were required, with a more conservative minimum coverage filter of 15× used for assessment of imputation accuracy.

Pigmentation profiles

We used the hIrisPlex-S system to predict hair, skin and eye colour in high-coverage ancient samples[98,99]. Diploid genotypes were called at the relevant variant sites and inputted into the hIrisPlex-S online tool (https://hirisplex.erasmusmc.nl). Imputed diploid genotypes (genotype probability >0.66) were also used for pigmentation prediction across the larger dataset of ancient genomes. Results are shown in Supplementary Table 12.

Population genetic analyses

Detailed descriptions for Y chromosome analysis, ADMIXTURE analysis[15], *D*- and *f*-statistics[100,101] using the AdmixTools package[102], ChromoPainter and fineSTRUCTURE analysis[13], estimations of runs of homozygosity, inbreeding coefficients and kinship determination with lcMLkin[26] can be found in Supplementary Information sections 2–6. We used smartpca[103,104] to construct the principal component analysis of SNP sharing in Extended Data Fig. 9a, using an identical sample and set of SNPs to that presented in Fig. 1d, e, with imputed genotypes converted randomly to homozygous to mimic pseudo-haploid data. Figures were produced in R[105] using the packages ggplot2[106], gplots[107], maps[108] and mapdata[109], with the reshape2[110] and dplyr[111] packages used for data manipulation.

Reporting summary

Further information on research design is available in the Nature Research Reporting Summary linked to this paper.

Data availability

Raw FASTQ and aligned BAM files are available through the European Nucleotide Archive under accession number PRJEB36854. Any other relevant data are available from the corresponding authors upon reasonable request.

35. Yang, D. Y., Eng, B., Waye, J. S., Dudar, J. C. & Saunders, S. R. Technical note: improved DNA extraction from ancient bones using silica-based spin columns. *Am. J. Phys. Anthropol.* **105**, 539–543 (1998).
36. MacHugh, D. E., Edwards, C. J., Bailey, J. F., Bancroft, D. R. & Bradley, D. G. The extraction and analysis of ancient DNA from bone and teeth: a survey of current methodologies. *Anc. Biomol.* **3**, 81–103 (2000).
37. Gamba, C. et al. Genome flux and stasis in a five millennium transect of European prehistory. *Nat. Commun.* **5**, 5257 (2014).
38. Meyer, M. & Kircher, M. Illumina sequencing library preparation for highly multiplexed target capture and sequencing. *Cold Spring Harb. Protoc.* **2010**, db.prot5448 (2010).
39. Andrews, S. FastQC: a quality control tool for high throughput sequence data. https://www.bioinformatics.babraham.ac.uk/projects/fastqc/ (2010).

40. Martin, M. Cutadapt removes adapter sequences from high-throughput sequencing reads. *EMBnet J.* **17**, 10–12 (2011).
41. Renaud, G., Stenzel, U. & Kelso, J. leeHom: adaptor trimming and merging for Illumina sequencing reads. *Nucleic Acids Res.* **42**, e141 (2014).
42. Li, H. & Durbin, R. Fast and accurate short read alignment with Burrows–Wheeler transform. *Bioinformatics* **25**, 1754–1760 (2009).
43. Li, H. et al. The Sequence Alignment/Map format and SAMtools. *Bioinformatics* **25**, 2078–2079 (2009).
44. McKenna, A. et al. The Genome Analysis Toolkit: a MapReduce framework for analyzing next-generation DNA sequencing data. *Genome Res.* **20**, 1297–1303 (2010).
45. Keller, A. et al. New insights into the Tyrolean Iceman's origin and phenotype as inferred by whole-genome sequencing. *Nat. Commun.* **3**, 698 (2012).
46. Olalde, I. et al. Derived immune and ancestral pigmentation alleles in a 7,000-year-old Mesolithic European. *Nature* **507**, 225–228 (2014).
47. Skoglund, P. et al. Genomic diversity and admixture differs for Stone-Age Scandinavian foragers and farmers. *Science* **344**, 747–750 (2014).
48. Allentoft, M. E. et al. Population genomics of Bronze Age Eurasia. *Nature* **522**, 167–172 (2015).
49. Günther, T. et al. Ancient genomes link early farmers from Atapuerca in Spain to modern-day Basques. *Proc. Natl Acad. Sci. USA* **112**, 11917–11922 (2015).
50. Haak, W. et al. Massive migration from the steppe was a source for Indo-European languages in Europe. *Nature* **522**, 207–211 (2015).
51. Jones, E. R. et al. Upper Palaeolithic genomes reveal deep roots of modern Eurasians. *Nat. Commun.* **6**, 8912 (2015).
52. Mathieson, I. et al. Genome-wide patterns of selection in 230 ancient Eurasians. *Nature* **528**, 499–503 (2015).
53. Olalde, I. et al. A common genetic origin for early farmers from Mediterranean Cardial and Central European LBK cultures. *Mol. Biol. Evol.* **32**, 3132–3142 (2015).
54. Broushaki, F. et al. Early Neolithic genomes from the eastern Fertile Crescent. *Science* **353**, 499–503 (2016).
55. Hofmanová, Z. et al. Early farmers from across Europe directly descended from Neolithic Aegeans. *Proc. Natl Acad. Sci. USA* **113**, 6886–6891 (2016).
56. Kılınç, G. M. et al. The demographic development of the first farmers in Anatolia. *Curr. Biol.* **26**, 2659–2666 (2016).
57. Jones, E. R. et al. The Neolithic transition in the Baltic was not driven by admixture with early European farmers. *Curr. Biol.* **27**, 576–582 (2017).
58. Schiffels, S. et al. Iron Age and Anglo-Saxon genomes from East England reveal British migration history. *Nat. Commun.* **7**, 10408 (2016).
59. Martiniano, R. et al. Genomic signals of migration and continuity in Britain before the Anglo-Saxons. *Nat. Commun.* **7**, 10326 (2016).
60. González-Fortes, G. et al. Paleogenomic Evidence for multi-generational mixing between Neolithic farmers and Mesolithic hunter-gatherers in the lower Danube basin. *Curr. Biol.* **27**, 1801–1810.e10 (2017).
61. Lipson, M. et al. Parallel palaeogenomic transects reveal complex genetic history of early European farmers. *Nature* **551**, 368–372 (2017).
62. Mathieson, I. et al. The genomic history of southeastern Europe. *Nature* **555**, 197–203 (2018).
63. Sánchez-Quinto, F. et al. Genomic affinities of two 7,000-year-old Iberian hunter-gatherers. *Curr. Biol.* **22**, 1494–1499 (2012).
64. Valdiosera, C. et al. Four millennia of Iberian biomolecular prehistory illustrate the impact of prehistoric migrations at the far end of Eurasia. *Proc. Natl Acad. Sci. USA* **115**, 3428–3433 (2018).
65. Günther, T. et al. Population genomics of Mesolithic Scandinavia: investigating early postglacial migration routes and high-latitude adaptation. *PLoS Biol.* **16**, e2003703 (2018).
66. Krzewińska, M. et al. Genomic and strontium isotope variation reveal immigration patterns in a Viking age town. *Curr. Biol.* **28**, 2730–2738.e10 (2018).
67. Krzewińska, M. et al. Ancient genomes suggest the eastern Pontic–Caspian steppe as the source of western Iron Age nomads. *Sci. Adv.* **4**, eaat4457 (2018).
68. Sikora, M. et al. Ancient genomes show social and reproductive behavior of early Upper Paleolithic foragers. *Science* **358**, 659–662 (2017).
69. Scheib, C. L. et al. East Anglian early Neolithic monument burial linked to contemporary megaliths. *Ann. Hum. Biol.* **46**, 145–149 (2019).
70. Saag, L. et al. Extensive farming in Estonia started through a sex-biased migration from the steppe. *Curr. Biol.* **27**, 2185–2193.e6 (2017).
71. Rodríguez-Varela, R. et al. Genomic analyses of pre-European conquest human remains from the Canary Islands reveal close affinity to modern North Africans. *Curr. Biol.* **28**, 1677–1679 (2018).
72. Reimer, P. J. et al. IntCal13 and Marine13 radiocarbon age calibration curves 0–50,000 years cal BP. *Radiocarbon* **55**, 1869–1887 (2013).
73. Eogan, G. *Excavations at Knowth Volume 6: The Passage Tomb Archaeology of the Great Mound at Knowth* (Royal Irish Academy, 2017).
74. Hamilton, J. & Hedges, R. E. M. in *Gathering Time: Dating the Early Neolithic Enclosures of Southern Britain and Ireland* (eds. Whittle, A. et al.) 670–681 (Oxbow Books, 2011).
75. Hutchison, M., Curtis, N. & Kidd, R. The Knowe of Rowiegar, Rousay, Orkney. *Proc. Soc. Antiquar. Scotland* **145**, 41–89 (2015).
76. Kador, T., Fibiger, L., Cooney, G. & Fullagar, P. Movement and diet in early Irish prehistory: first evidence from multi-isotope analysis. *J. Irish Archaeol.* **23**, 83–96 (2015).
77. Schulting, R. in *The Origins and Spread of Domestic Animals in Southwest Asia and Europe* (eds. Colledge, S. et al.) 313–338 (2013).
78. Schulting, R. J., Murphy, E., Jones, C. & Warren, G. New dates from the north and a proposed chronology for Irish court tombs. *Proc. R. Ir. Acad. C Archaeol. Celt. Stud. Hist. Linguist. Lit.* **112C**, 1–60 (2012).
79. Wysocki, M. et al. Dates, diet, and dismemberment: evidence from the Coldrum megalithic monument, Kent. *Proc. Prehist. Soc.* **79**, 61–90 (2013).
80. Wysocki, M., Bayliss, A. & Whittle, A. serious mortality: the date of the Fussell's Lodge long barrow. *Camb. Archaeol. J.* **17**, 65–84 (2007).

81. Whittle, A. et al. Parc le Breos Cwm transepted long cairn, Gower, West Glamorgan: date, contents, and context. *Proc. Prehist. Soc.* **64**, 139–182 (1998).

82. Whittle, A., Bayliss, A. & Wysocki, M. Once in a lifetime: the date of the Wayland's Smithy long barrow. *Camb. Archaeol. J.* **17**, 103–121 (2007).

83. Bayliss, A., Whittle, A. & Wysocki, M. Talking about my generation: the date of the West Kennet long barrow. *Camb. Archaeol. J.* **17**, 85–101 (2007).

84. Brindley, A. L., Lanting, J. N. & van der Plicht, J. in *Duma na nGial: The Mound of the Hostages, Tara* (ed. O'Sullivan, M.) 281–296 (Wordwell, 2005).

85. Schulting, R. J., Chapman, M. & Chapman, E. J. AMS ¹⁴C dating and stable isotope (carbon, nitrogen) analysis of an earlier Neolithic human skeletal assemblage from hay wood cave, Mendip, Somerset. *Proc. Univ. Bristol Spelaeol. Soc.* **26**, 9–26 (2013).

86. Schulting, R. et al. Mesolithic and Neolithic human remains from Foxhole Cave, Gower, South Wales. *Antiq. J.* **93**, 1–23 (2013).

87. Sheridan, J. A., Schulting, R., Quinnell, H. & Taylor, R. Revisiting a small passage tomb at Broadsands, Devon. *Proc. Devon Archaeol. Soc.* **66**, 1–26 (2008).

88. Schulting, R. J. & Richards, M. P. Finding the coastal Mesolithic in southwest Britain: AMS dates and stable isotope results on human remains from Caldey Island, South Wales. *Antiquity* **76**, 1011–1025 (2002).

89. Stevens, R. E., Lightfoot, E., Allen, T. & Hedges, R. E. M. Palaeodiet at Eton College rowing course, Buckinghamshire: isotopic changes in human diet in the Neolithic, Bronze Age, Iron Age and Roman periods throughout the British Isles. *Archaeol. Anthropol. Sci.* **4**, 167–184 (2012).

90. Chamberlain, A. T. & Witkin, A. V. A Neolithic cairn at Whitwell, Derbyshire. *Derbyshire Archaeol. J.* **131**, 1–131 (2011).

91. McLaughlin, T. R., Whitehouse, N. J. & Schulting, R. J. The changing face of Neolithic and Bronze Age Ireland: a big data approach to the settlement and burial records. *J. World Prehist.* **29**, 117–153 (2016).

92. Skoglund, P., Storå, J., Götherström, A. & Jakobsson, M. Accurate sex identification of ancient human remains using DNA shotgun sequencing. *J. Archaeol. Sci.* **40**, 4477–4482 (2013).

93. Okonechnikov, K., Conesa, A. & García-Alcalde, F. Qualimap 2: advanced multi-sample quality control for high-throughput sequencing data. *Bioinformatics* **32**, 292–294 (2016).

94. Vianello, D. et al. HAPLOFIND: a new method for high-throughput mtDNA haplogroup assignment. *Hum. Mutat.* **34**, 1189–1194 (2013).

95. Browning, S. R. & Browning, B. L. Rapid and accurate haplotype phasing and missing-data inference for whole-genome association studies by use of localized haplotype clustering. *Am. J. Hum. Genet.* **81**, 1084–1097 (2007).

96. Gallego-Llorente, M. et al. The genetics of an early Neolithic pastoralist from the Zagros, Iran. *Sci. Rep.* **6**, 31326 (2016).

97. The 1000 Genomes Project Consortium et al. A global reference for human genetic variation. *Nature* **526**, 68–74 (2015).

98. Walsh, S. et al. The HIrisPlex system for simultaneous prediction of hair and eye colour from DNA. *Forensic Sci. Int. Genet.* **7**, 98–115 (2013).

99. Chaitanya, L. et al. The HIrisPlex-S system for eye, hair and skin colour prediction from DNA: introduction and forensic developmental validation. *Forensic Sci. Int. Genet.* **35**, 123–135 (2018).

100. Green, R. E. et al. A draft sequence of the Neandertal genome. *Science* **328**, 710–722 (2010).

101. Reich, D., Thangaraj, K., Patterson, N., Price, A. L. & Singh, L. Reconstructing Indian population history. *Nature* **461**, 489–494 (2009).

102. Patterson, N. et al. Ancient admixture in human history. *Genetics* **192**, 1065–1093 (2012).

103. Patterson, N., Price, A. L. & Reich, D. Population structure and eigenanalysis. *PLoS Genet.* **2**, e190 (2006).

104. Price, A. L. et al. Principal components analysis corrects for stratification in genome-wide association studies. *Nat. Genet.* **38**, 904–909 (2006).

105. R Core Team. *R: A Language and Environment for Statistical Computing* (R Foundation for Statistical Computing, 2015).

106. Wickham, H. *ggplot2: Elegant Graphics for Data Analysis* (Springer, 2016).

107. Warnes, G. R. et al. gplots: various R programming tools for plotting data, R package version 3.0.1, http://CRAN.R-project.org/package=gplots (2016).

108. Becker, R. A., Wilks, A. R., Brownrigg, R., Minka, T. P. & Deckmyn, A. maps: draw geographical maps, R package version 3.1.0. http://CRAN.R-project.org/package=maps (2016).

109. Becker, R. A., Brownrigg, R. & Wilks, A. R. mapdata: extra map databases, R package version 2.2-6, http://CRAN.R-project.org/package=mapdata (2016).

110. Wickham, H. Reshaping data with the reshape package. *J. Stat. Softw.* **21**, 1–20 (2007).

111. Wickham, H., François, R., Henry, L. & Müller, K. dplyr: a grammar of data manipulation, R package version 0.7.6, http://CRAN.R-project.org/package=dplyr (2018).

Author contributions D.G.B. and L.M.C. designed this study. L.M.C., V.M., A.N. and C.C. performed laboratory work. L.M.C. processed and analysed data with contributions from E.R.J. R.Ó M., T.K., A.L., C.J., P.C.W., E.M., G.R. and M.D. provided access to samples and supplied archaeological information and interpretation. L.M.C. and D.G.B. co-wrote the manuscript with input from all authors.

**Competing interests** The authors declare no competing interests.

Additional information
Supplementary information is available for this paper at https://doi.org/10.1038/s41586-020-2378-6.
Correspondence and requests for materials should be addressed to L.M.C. or D.G.B.
Peer review information *Nature* thanks Duncan Garrow, Michael Hofreiter and David Reich for their contribution to the peer review of this work.
**Reprints and permissions information** is available at http://www.nature.com/reprints.
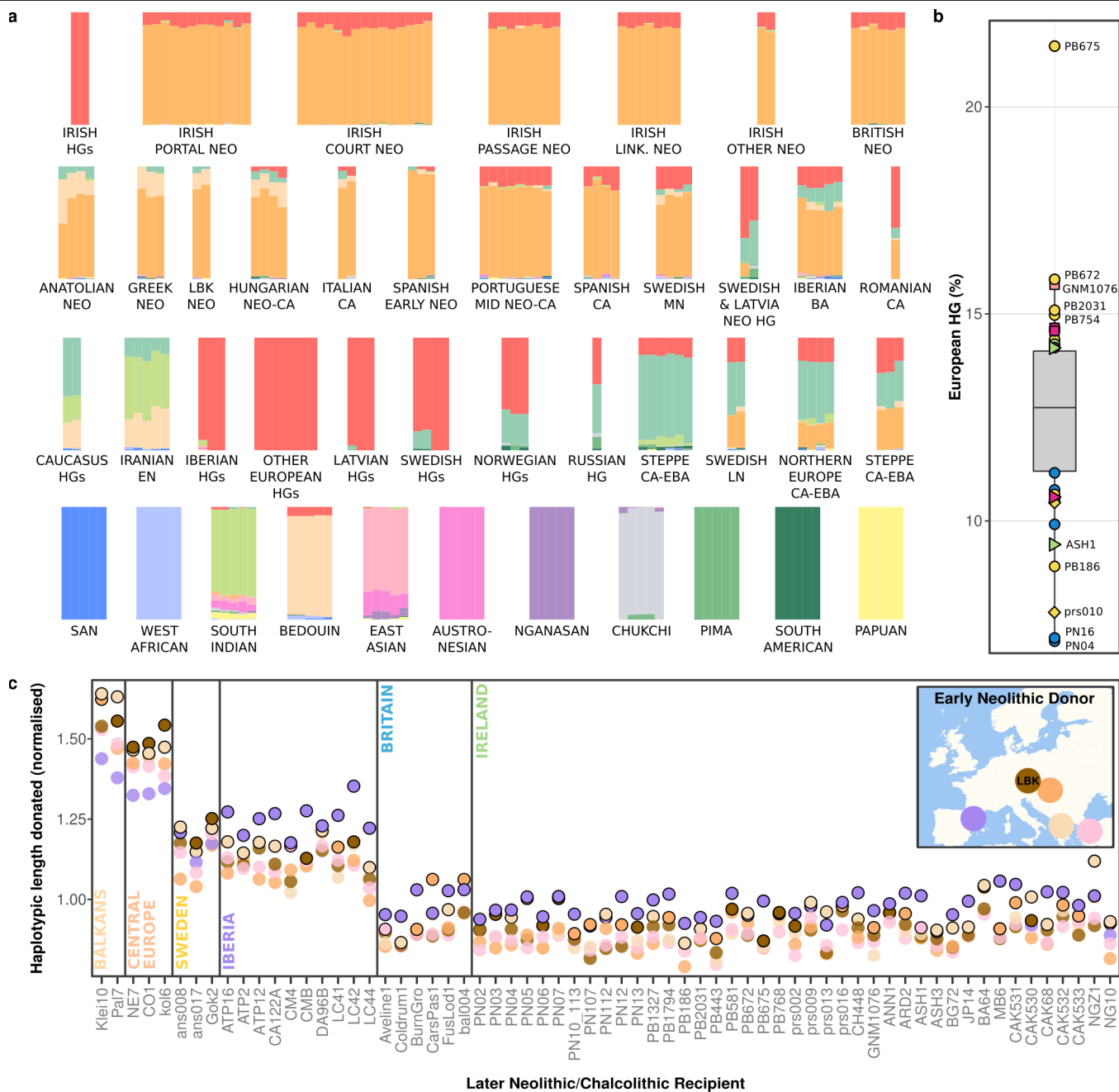
**Extended Data Fig. 1 | Genomic affinities of the Irish Neolithic.**
a, ADMIXTURE plot ($K = 14$) for ancient Irish and British populations (first row), other ancient Eurasians (second and third rows) and global modern populations (fourth row). For components that reach their maximum in modern populations, the five individuals with highest values were selected for representation. If the majority of these individuals come from a single population the block is labelled as such; otherwise, it is labelled using the general geographic region from which these individuals originate. Three components reach their maximum in ancient populations, and we label these 'European_HG' (red), Early_Farmer (orange) and 'Steppe' (teal). **b**, Box plot (Tukey method) showing the distribution of the European_HG component among British and Irish Neolithic shotgun-sequenced individuals ($n = 50$). **c**, Normalized haplotypic length contributions, estimated with ChromoPainter, from Early Neolithic populations to later Neolithic and Chalcolithic individuals. The top two donors are outlined in black for each individual. Given the unsupervised nature of the analysis, regional differences in overall haplotypic donation levels should be ignored, as larger populations have more opportunity for within-group painting.
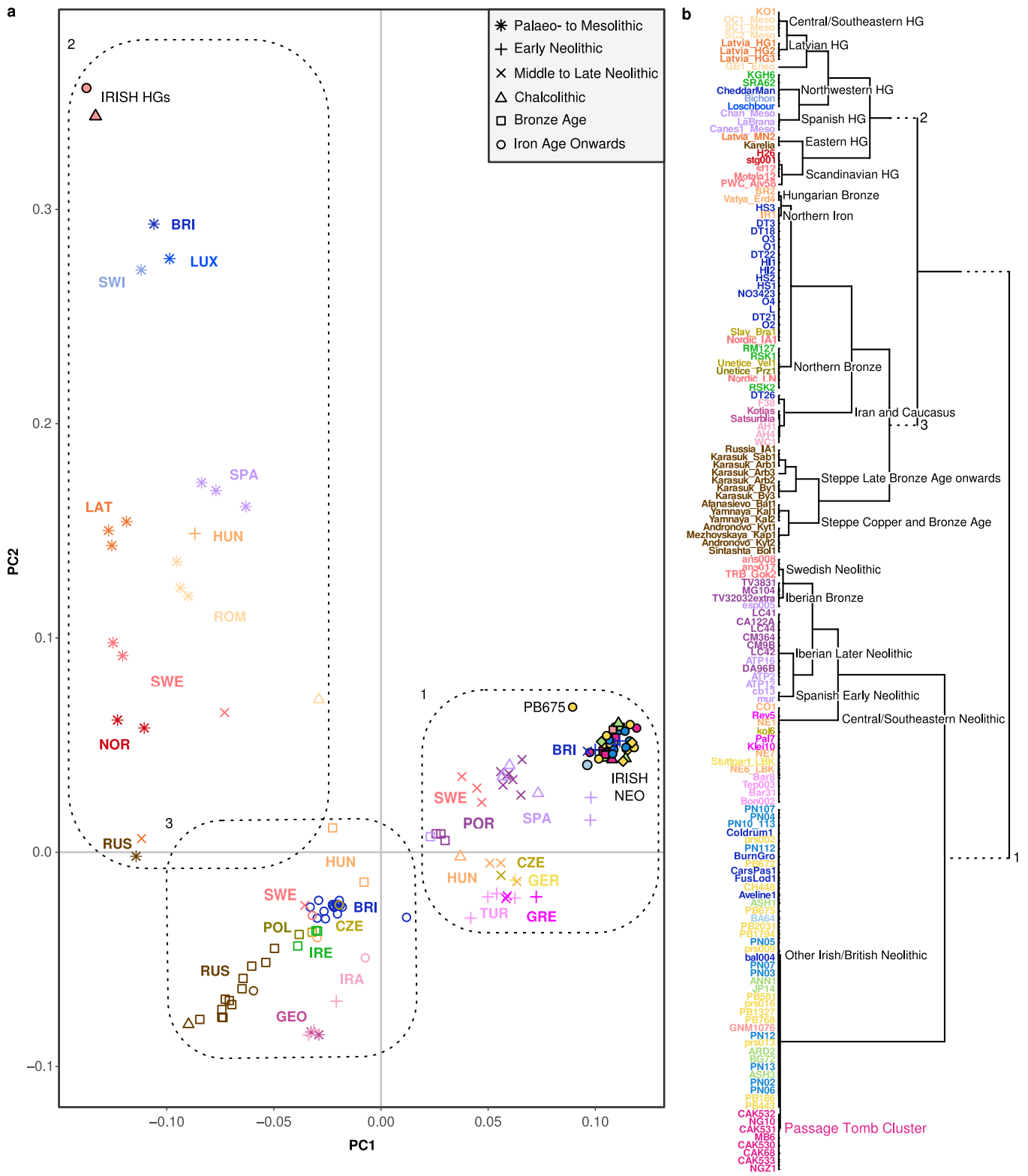
Extended Data Fig. 2 | Haplotypic structure among ancient populations. **a**, ChromoPainter principal component analysis of diverse ancient genomes (*n* = 149) generated using the output matrix of haplotypic lengths. The colour and shape key for the Irish samples follows Fig. 1. **b**, fineSTRUCTURE dendrogram derived from the same matrix as in **a**, with the passage tomb cluster highlighted. Dotted branches are shown at a quarter of their true length.
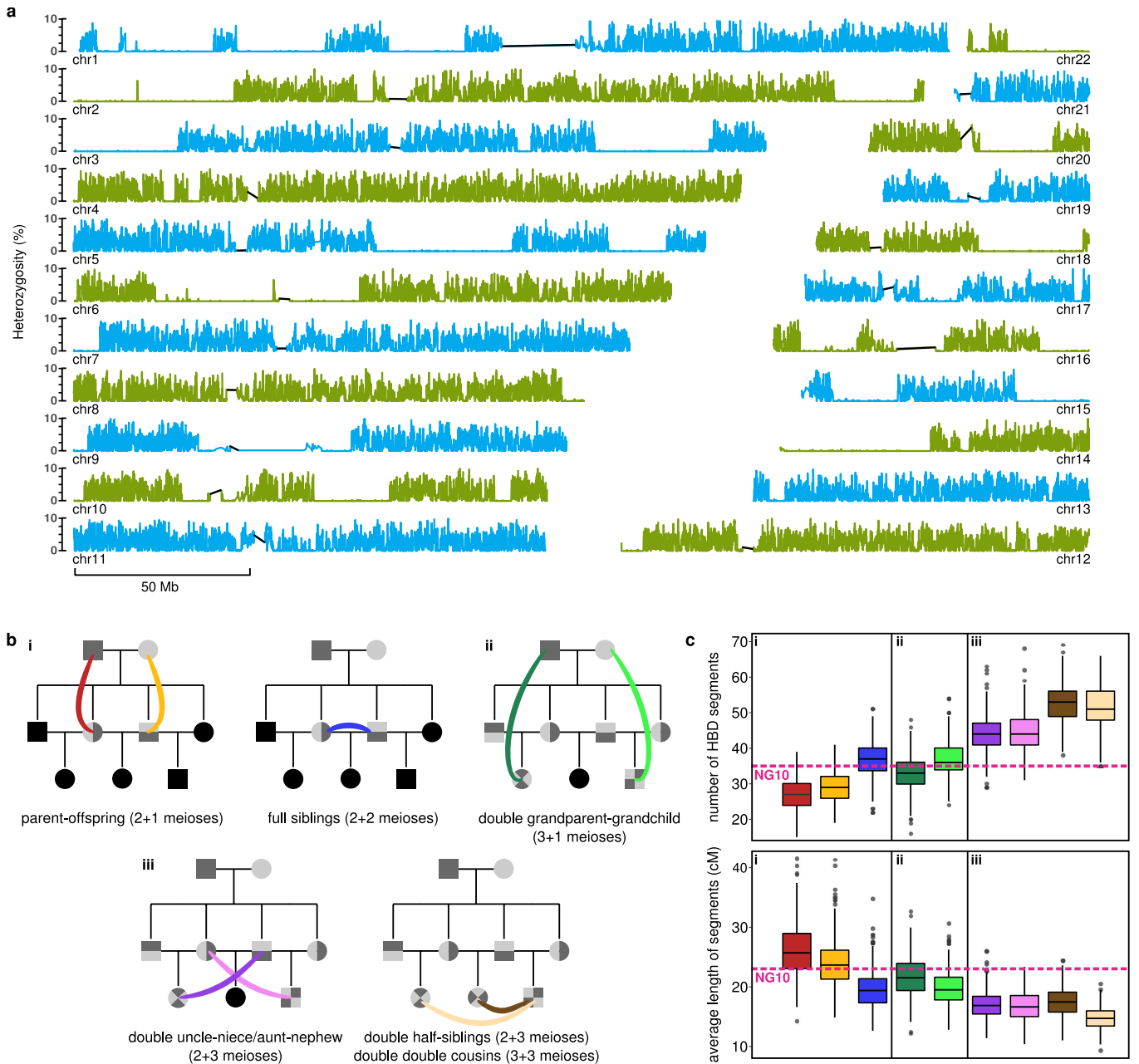
Extended Data Fig. 3 | Inferring the relationship between the parents of NG10. a, Whole-genome plot of heterozygosity in NG10, revealing extreme runs of homozygosity. **b**, Nine mating scenarios (coloured lines) that can lead to an inbreeding coefficient of 25%. **c**, Number and average lengths of homozygous-by-descent (HBD) segments for each of these simulated scenarios (500 iterations) and the same values observed for the NG10 genome. Box plots follow Tukey's method. Scenarios in the subpanels i and ii best fit the homozygous-by-descent distribution of NG10; ii is less parsimonious than i when anthropological and biological factors are taken into consideration.
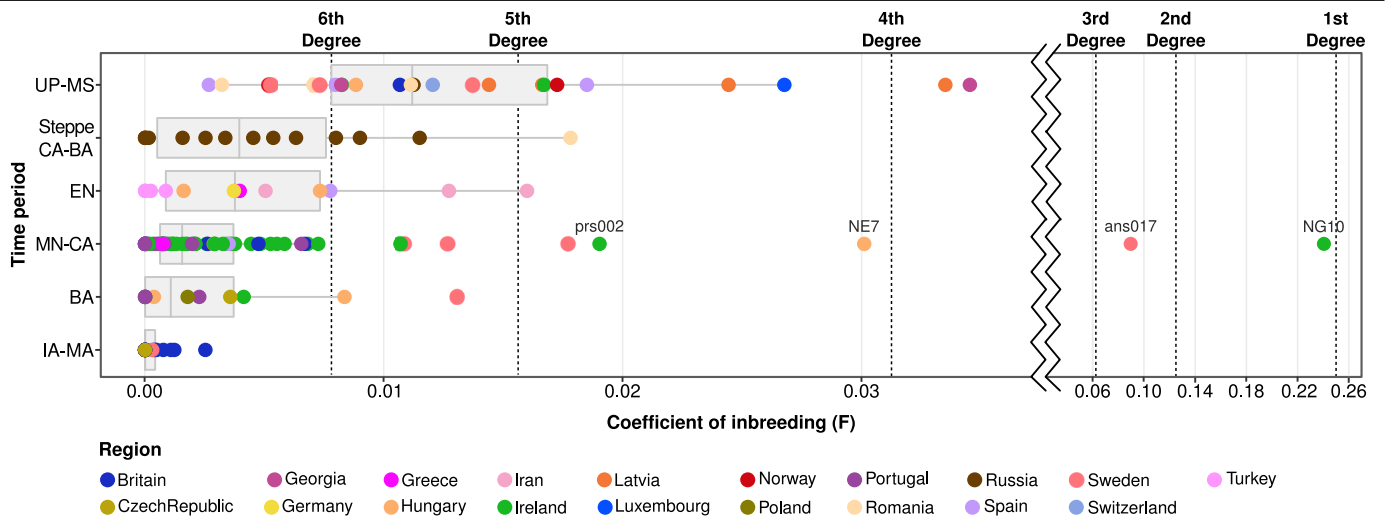
Extended Data Fig. 4 | Levels of inbreeding through time in ancient populations. Inbreeding coefficients for imputed ancient samples estimated by measuring the proportion of the genome that is homozygous by descent. Box plots follow Tukey's method. Individuals are binned according to archaeological period. UP-MS, Upper Palaeolithic to Mesolithic ($n = 24$); EN, Early Neolithic ($n = 13$); MN-CA, Middle Neolithic to Chalcolithic ($n = 69$); BA, European Bronze Age ($n = 12$); IA-MA, Iron Age to Medieval ($n = 21$); Steppe CA-BA, steppe Chalcolithic to Bronze Age ($n = 14$). Outliers of note are labelled. The inferred degrees of relatedness between the parents of an individual are marked.
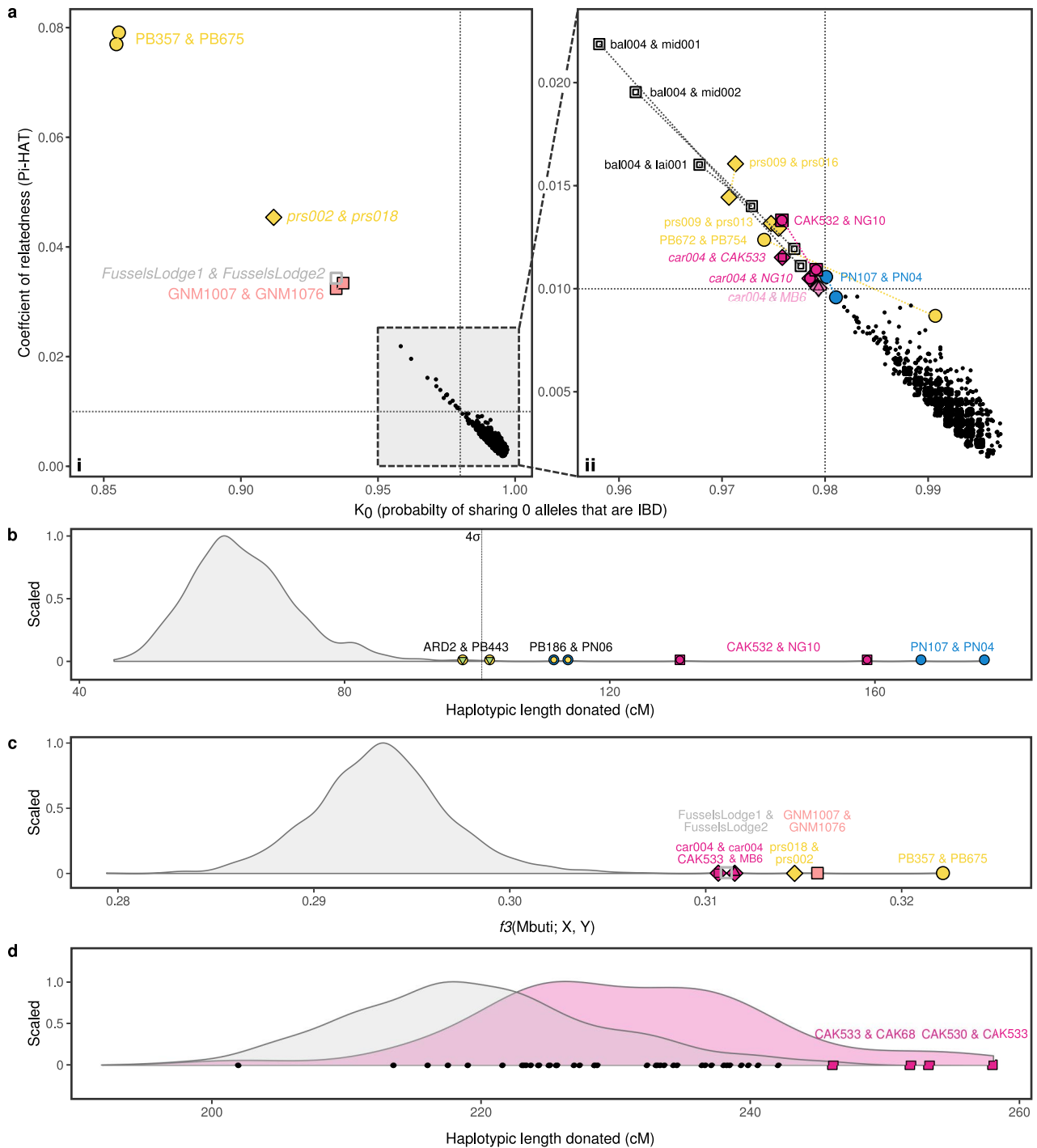
Extended Data Fig. 5 | Detecting recent shared ancestry between pairs of British and Irish Neolithic samples. a, lcMLkin[31] kinship coefficients between pairs of Irish and British Neolithic samples, jittered by a height of 0.00018 and width of 0.00036 for visualization. Optimized duplicate tests are linked by dotted lines. Several standalone values are also shown (italics), in which one duplicate did not meet the threshold of overlapping sites (>20,000). The MB6 and car004 pairing (19,850 sites) is shown as a translucent point. An inset is shown for lower values of pi-HAT. Pairs over 5σ from the mean pi-HAT and K_0 for subpanel ii (marked with a line) are highlighted using the same colour and shape key as in Fig. 1. Combined symbols are used for inter-site pairs. **b**, Total haplotypic lengths donated between all pairs ($n = 2,162$) of British and Irish samples from the ChromoPainter analysis of diverse ancient samples (Extended Data Fig. 2). Outlying pairs (4σ above the mean) are labelled. **c**, Outgroup f_3-statistics measuring shared drift between pairs ($n = 2,236$) of Irish and British Neolithic samples (>25,000 informative sites). **d**, Total haplotypic lengths donated between all pairs of 'passage tomb cluster' (pink; $n = 42$) and 'British–Irish cluster' (grey; $n = 1,190$) samples from the ChromoPainter analysis of genomes from the Atlantic seaboard (Fig. 1d, e). Single members from the outlying pairs in **b** were removed for this analysis. Positions of passage tomb pairs are marked along the x axis, with two outlying pairs from Carrowkeel highlighted.
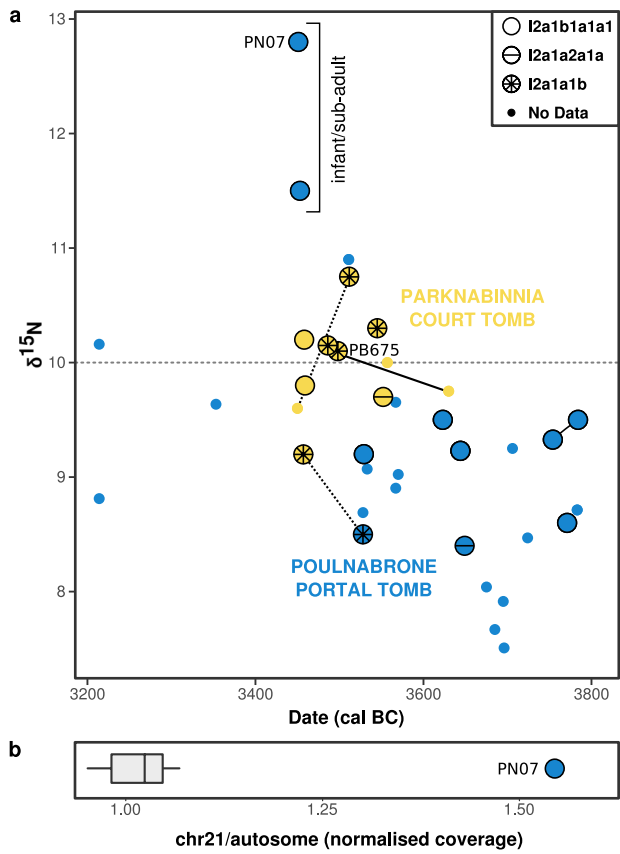
Extended Data Fig. 6 | Regional-scale diversity in the Irish Neolithic.
a, Nitrogen stable-isotope values (an indicator of trophic level) plotted across time for samples from the neighbouring sites of Poulnabrone (blue) and Parknabinnia (yellow). For male samples, the Y chromosome haplogroup is given. Distant kinship connections are marked with a dotted line, and a closer (about fourth degree) relationship is highlighted with a solid line. **b**, Box plot (Tukey's method) of normalized read coverage aligning to chromosome 21 for shotgun-sequenced ancient samples ($n = 188$), with a single outlier from Poulnabrone (representing an infant with trisomy).
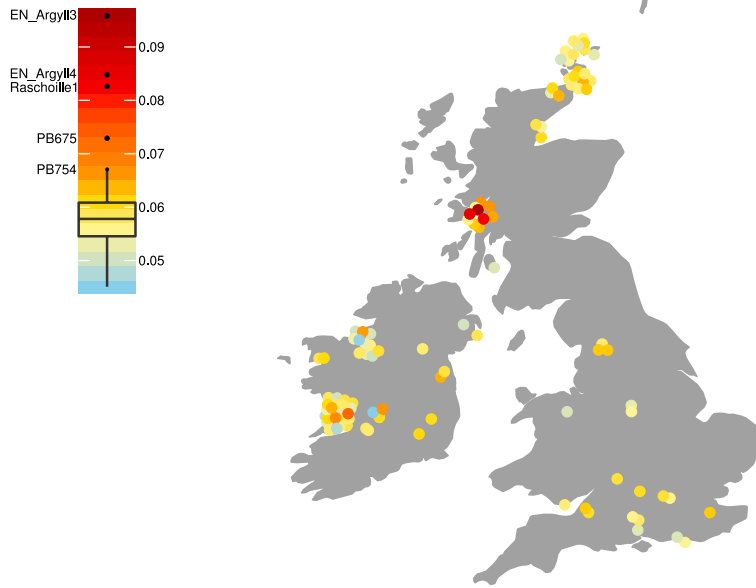
Article
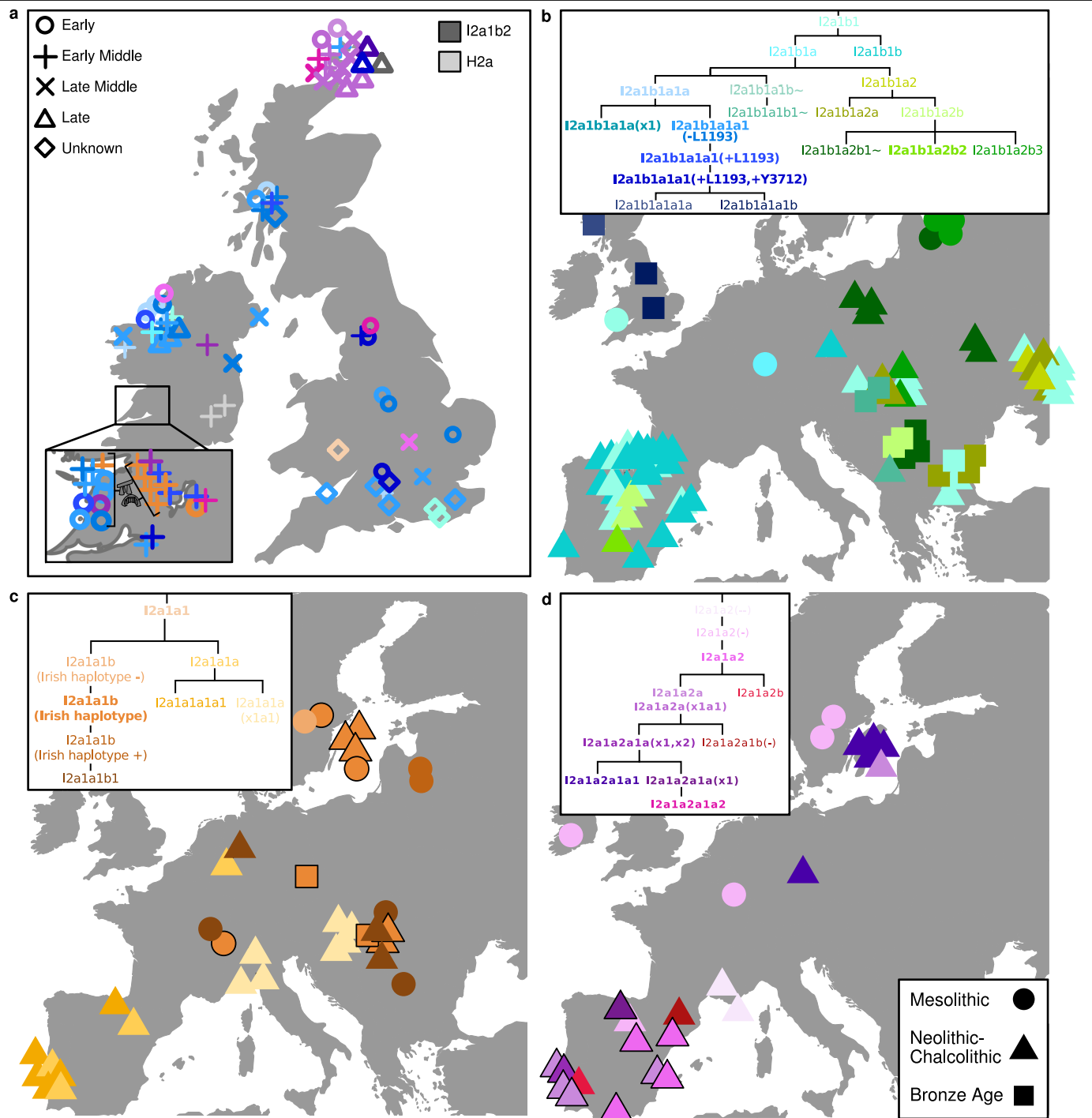
Extended Data Fig. 7 | Subclade distributions of Y chromosome haplogroup I2a1 in Ireland, Britain and Europe from the Mesolithic to the Bronze Age.
a, Y haplogroups observed for Neolithic individuals (jittered) in Britain and Ireland. Shape indicates the approximate time period within the Neolithic (based on ref. [91]), and colour indicates haplogroup and follows the same keys as in **b**–**d**. **b**–**d**, Approximately 94% of the British and Irish Neolithic samples belong to haplogroups I2a1b1 (45%), I2a1a1 (14%) and I2a1a2 (35%). Incidences

(jittered) of these haplogroups in European individuals from the Mesolithic to the Bronze Age are shown for I2a1b1 (**b**), I2a1a1 (**c**) and I2a1a2 (**d**). Haplogroup colour keys are shown with respect to phylogenetic placement; those haplogroups observed within Britain and Ireland are shown in bold. European individuals who share an identical set of haplotypic mutations (for sites covered) to an Irish Neolithic individual are highlighted with a black outline in **c** (for I2a1a1) and **d** (for I2a1a2).
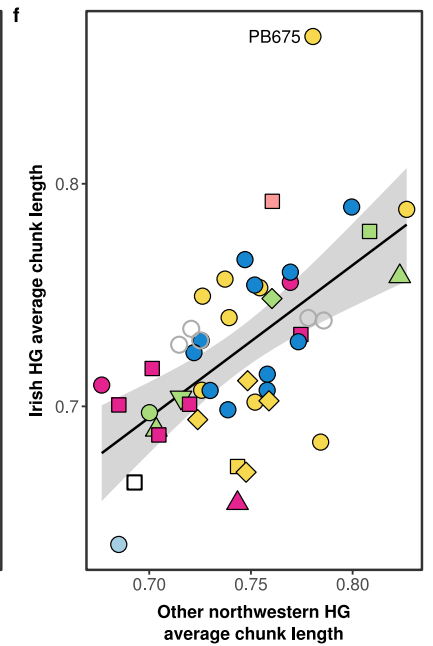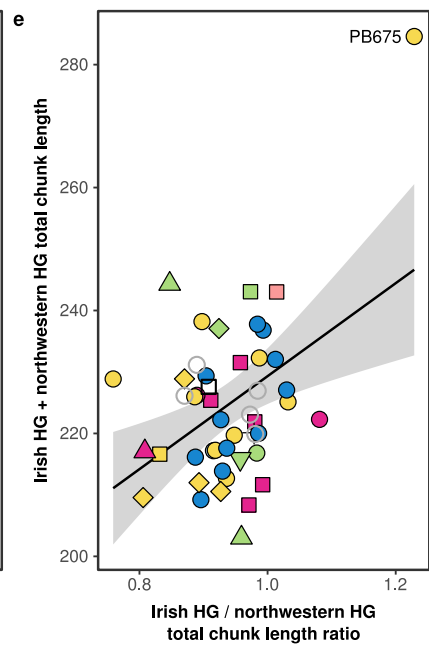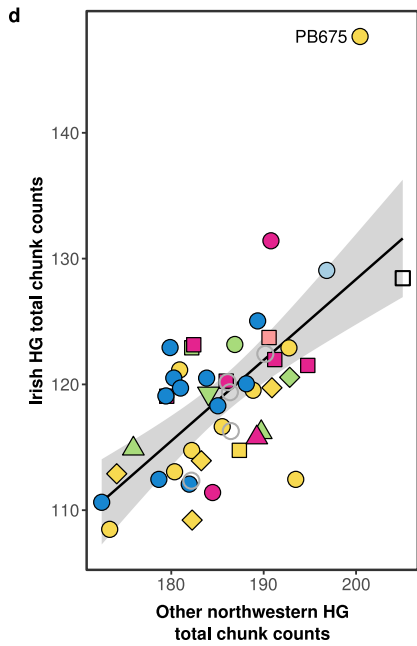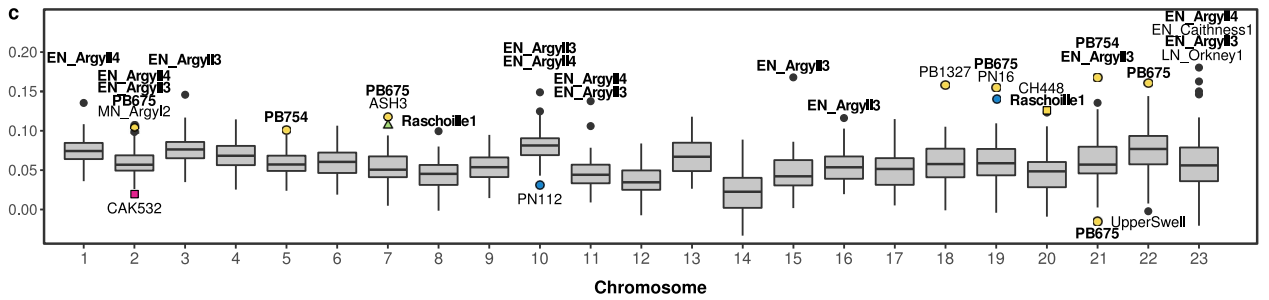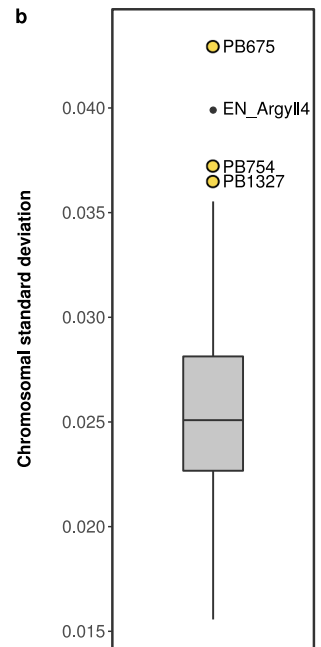
**Extended Data Fig. 8** | See next page for caption.

Article

Extended Data Fig. 8 | Geographic and genomic distributions of northwestern European hunter-gatherer ancestry among British and Irish Neolithic individuals. a, Geographic distribution of northwestern European hunter-gatherer introgression in Britain and Ireland across 103 Neolithic samples. Box plot (Tukey's method) highlights four outliers, three from the Early-to-Middle Neolithic of Argyll and one from Ireland (designated Parknabinnia675 (PB675)). The next highest value is also from Parknabinnia (individual PB754). **b**, The same *D*-statistic run on separate chromosomes for individuals of sufficient coverage ($n = 86$). Outlying individuals are marked for each chromosome. Irish outliers follow the same shape and colour key as in Fig. 1. Outliers who are also outliers in the box plot in **a** are marked in bold. **c**, Box plot (Tukey's method; $n = 86$) of sample standard deviations across the chromosomes for the same *D*-statistic. Four outliers with high variance across the chromosomes are marked, including three samples from Parknabinnia, two of whom are also top hits in **a**. **d**–**f**, Haplotypic affinities of imputed Irish and British Neolithic individuals ($n = 47$) to Irish hunter-gatherers, relative to other northwestern European hunter-gatherers (Bichon, Loschbour and Cheddar Man). Colour and shape key follows Fig. 1. The outlying individual PB675 shows a preference for Irish hunter-gatherer haplotypes in all measures. Regression lines are shown with 95% confidence interval shaded (sample size = 47). PB675 shows a higher-than-expected number of Irish hunter-gatherer haplotypes (**d**), has the highest overall hunter-gatherer haplotypic length contribution, with a ratio skewed towards Irish hunter-gatherers (**e**) and displays the longest average length of Irish-hunter-gatherer haplotype chunks (**f**).
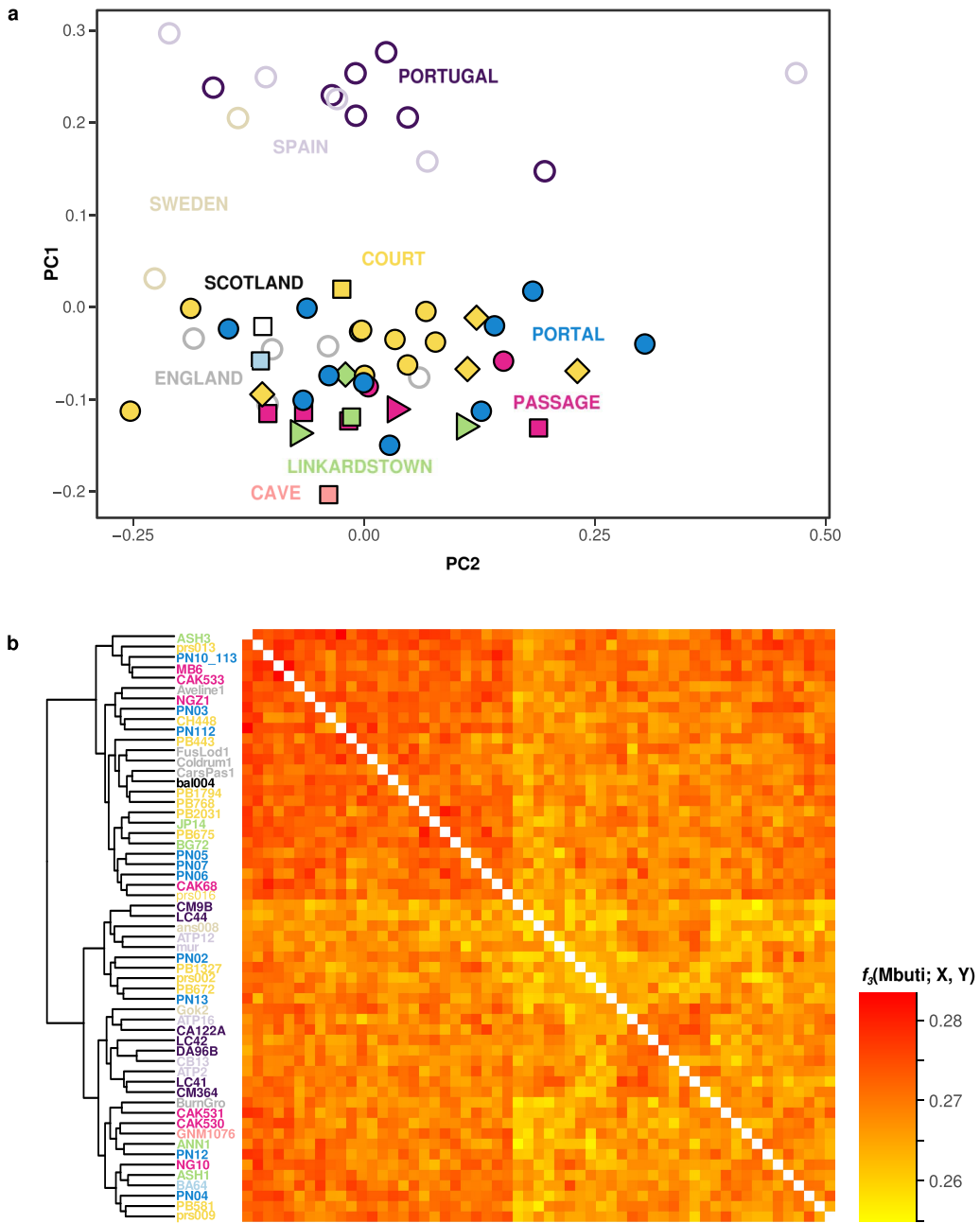
Extended Data Fig. 9 | SNP-sharing analyses of autosomal structure in Neolithic populations of the Atlantic seaboard. a, Principal component analysis created using an identical sample ($n = 57$) and set of SNPs (about 488,000 sites; pseudo-haplodized) to that presented in Fig. 1d, e. **b**, Outgroup f_3-statistics for all combinations of samples in **a**, using a reduced set of SNPs (about 270,000 sites; pseudo-haplodized). Results are presented in a heat map and corresponding dendrogram.
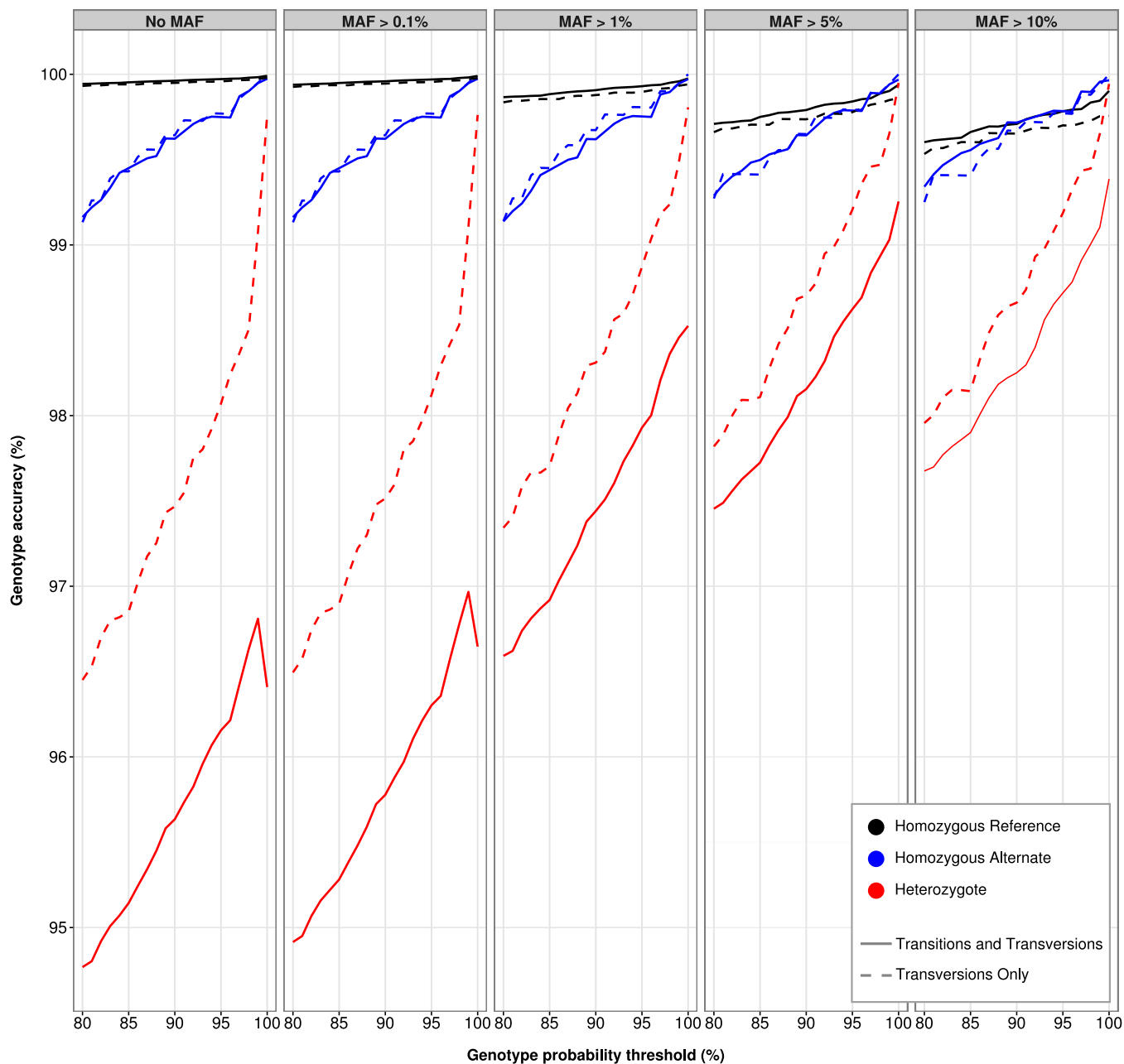
Extended Data Fig. 10 | Imputation accuracies for chromosome 22 of the high-coverage NE1 genome, downsampled to 1×. The levels of accuracy seen across all SNPs (solid line) ($n = 204,316$ for no minor allele frequency (MAF) filter and genotype probability of 80) is compared to that seen for transversions only (dashed line) ($n = 62,374$ for no minor allele frequency filter and genotype probability of 80). Accuracies at different genotype probability thresholds and minor allele frequency filters are shown for the three different genotype categories. Minor allele frequency filters are based on overall frequency in the 1000 Genomes phase 3 dataset.

naturereseach

Corresponding author(s): Daniel G Bradley and Lara M Cassidy

Last updated by author(s): Mar 1, 2020

Reporting Summary

Nature Research wishes to improve the reproducibility of the work that we publish. This form provides structure for consistency and transparency in reporting. For further information on Nature Research policies, see Authors & Referees and the Editorial Policy Checklist.

Statistics

For all statistical analyses, confirm that the following items are present in the figure legend, table legend, main text, or Methods section.

n/a	Confirmed	
☐	☒	The exact sample size (*n*) for each experimental group/condition, given as a discrete number and unit of measurement
☐	☒	A statement on whether measurements were taken from distinct samples or whether the same sample was measured repeatedly
☐	☒	The statistical test(s) used AND whether they are one- or two-sided *Only common tests should be described solely by name; describe more complex techniques in the Methods section.*
☐	☒	A description of all covariates tested
☐	☒	A description of any assumptions or corrections, such as tests of normality and adjustment for multiple comparisons
☐	☒	A full description of the statistical parameters including central tendency (e.g. means) or other basic estimates (e.g. regression coefficient) AND variation (e.g. standard deviation) or associated estimates of uncertainty (e.g. confidence intervals)
☐	☒	For null hypothesis testing, the test statistic (e.g. *F*, *t*, *r*) with confidence intervals, effect sizes, degrees of freedom and *P* value noted *Give P values as exact values whenever suitable.*
☐	☒	For Bayesian analysis, information on the choice of priors and Markov chain Monte Carlo settings
☒	☐	For hierarchical and complex designs, identification of the appropriate level for tests and full reporting of outcomes
☒	☐	Estimates of effect sizes (e.g. Cohen's *d*, Pearson's *r*), indicating how they were calculated

Our web collection on statistics for biologists contains articles on many of the points above.

Software and code

Policy information about availability of computer code

Data collection	Calib (v7.1) FASTQC (v0.11.5) cutadapt (v.2.1 and v1.9.1) bwa (v0.7.12 and v0.7.13) samtools (v0.1.19, v1.3 and v1.7) picard tools (v1.101) beagle (4.0) GATK (v2.4 and v4.0.11) convertf (v4480) shapeit (v2.r837) PLINK (v1.9)
Data analysis	HaploFind (haplofind.unibo.it) Chromopainter and fineSTRUCTURE (v2) with accompanying R packages (FinestructureRcode.zip) ADMIXTURE (v1.2) Qualimap (v2.1.1) PLINK (v1.9) lcmlkin (v0.5.0) with accompanying SNPbam2vcf.py script ADMIXTOOLS version 3.0 - qp3pop (v300) and qpDstat (v662) EIGENSOFT version 3.0 - smartpca (v8000) R software (packages: ggplot2, gplots, maps, dplyr, reshape2) hIrisPlex-S (https://hirisplex.erasmusmc.nl)

For manuscripts utilizing custom algorithms or software that are central to the research but not yet described in published literature, software must be made available to editors/reviewers. We strongly encourage code deposition in a community repository (e.g. GitHub). See the Nature Research guidelines for submitting code & software for further information.

Data

All manuscripts must include a [data availability statement](#). This statement should provide the following information, where applicable:

- Accession codes, unique identifiers, or web links for publicly available datasets
- A list of figures that have associated raw data
- A description of any restrictions on data availability

> Raw and aligned data are available through the European Nucleotide Archive under accession number PRJEB36854

Field-specific reporting

Please select the one below that is the best fit for your research. If you are not sure, read the appropriate sections before making your selection.

☒ Life sciences ☐ Behavioural & social sciences ☐ Ecological, evolutionary & environmental sciences

For a reference copy of the document with all sections, see [nature.com/documents/nr-reporting-summary-flat.pdf](#)

Life sciences study design

All studies must disclose on these points even when the disclosure is negative.

Sample size	Sample size was not predetermined. We sampled and sequenced as many Mesolithic and Neolithic specimens from Ireland as were accessible and of sufficient preservation. The sample size is typical for studies of ancient populations. The sample size is sufficient for all conclusions drawn.
Data exclusions	Ancient samples with endogenous contents below 5% or concentrations below 0.5 ng/ul were excluded from higher coverage sequencing. These criteria were pre-established within laboratory pipelines. Quality and coverage thresholds were applied in a number of analyses, details of which are found in the methods section.
Replication	Replication is not applicable to studies of unique ancient specimens.
Randomization	We grouped samples based on archaeological context, date and ancestry. No randomisation was performed.
Blinding	No blinding was performed. There was no difference in sample processing or treatment across the dataset.

Reporting for specific materials, systems and methods

We require information from authors about some types of materials, experimental systems and methods used in many studies. Here, indicate whether each material, system or method listed is relevant to your study. If you are not sure if a list item applies to your research, read the appropriate section before selecting a response.

Materials & experimental systems

n/a	Involved in the study
☒	Antibodies
☒	Eukaryotic cell lines
☒	Palaeontology
☒	Animals and other organisms
☒	Human research participants
☒	Clinical data

Methods

n/a	Involved in the study
☒	ChIP-seq
☒	Flow cytometry
☒	MRI-based neuroimaging